

Chapter 6

Discussion

Subduction zones are the locations on the surface of the Earth along which chemically different materials are introduced into the mantle. Despite numerous studies in this particular setting, many important chemical aspects of the subduction processes and materials that affect mantle geochemistry are poorly understood. In this work we have tried to resolve some of the important issues related to the chemical evolution of the mantle at subduction zones with a focus on chemical characterization of subducting materials, suprasubduction ophiolites and island arc lavas.

The Andaman subduction zone was chosen as our study area because it is one of the few accretionary convergent margins where all the important components of a convergent margin are exposed and are available for scientific scrutiny. These include a trench, an outer arc accretionary prism, a forearc, a volcanic arc, and a back arc basin. To understand the subduction zone processes, crust – mantle interaction and origin and evolution of arc magmas, we examined the three most important components of the subduction zone. To answer the questions pertaining to the initiation of subduction we focussed on the study of the Ophiolite Group, whereas answers to questions on chemistry of subducting materials came from the study of fluids and solid materials emitted from the mud volcanoes located on the accretionary prism. To understand the evolution of the arc mantle melting in the mantle wedge we focussed our study on the lavas and ash beds from the Barren Island Volcano. In the following paragraphs, I discuss the results of our field and experimental studies and use various mixing and melting models to provide answers to the questions that I formulated for this thesis work on the origin and evolution of the Andaman subduction zone.

6.1 Origin of Andaman Ophiolites

6.1.1 Inferences from field relationships and Petrography

The Ophiolite suites of Andaman consist of a plutonic complex, a volcanic sequence and pelagic sedimentary rocks. The lower part of the group (80% of the total outcrop) comprises foliated and highly serpentized peridotite. The upper part comprises a layered sequence of ultramafic–mafic rocks, an intrusive section of homogeneous gabbro–plagiogranite–diorite–dolerite and an extrusive section of boninite and tholeiitic basalt lavas. Although ophiolite occurrences are reported from almost all the major Andaman Islands, the greatest numbers of ophiolites slices are present in South Andaman island, where the largest slices range in thickness from 300 to 750 m, but the largest volume of mantle sequences are exposed in Middle and North Andaman islands (Pal et al., 2003). Pal (2011) divided ophiolites suite into five parts; I) mantle tectonite (deformed and serpentized lherzolites and harzburgites), II) layered ultramafic - mafic sequences (dunite, lherzolite, gabbro-pyroxinite), III) intrusive units (gabbro, plagiogranite, dolerite), IV) extrusive units (pillow basalt) and V) sedimentary cover (oceanic-pelagic sediment, ophiolite derived clastics, rhythmite and olistostromal argillaceous sediment).

The following inferences can be made from our field observations, which somewhat are in agreements with the inferences drawn by earlier workers about the evolution of this sequence.

I) Although the ophiolite sequence appears to be complete with all its members, all the members are not exposed at a single location suggesting that the sequence got dismembered prior to their emplacement close to the surface.

II) The ophiolites form the basement of the accretionary wedge ruling out the possibility of them being an obducted portion of the slab. This might indicate that these were formed at the subduction zone itself.

The photomicrographs of thin sections of Andaman igneous rocks have already been presented in the last chapter. Our petrographical study on Andaman samples reveals that the most of the samples are highly altered with most samples being serpentinized. The predominant rock type amongst the magmatic rocks in the Andaman Ophiolites is basalt. In the thin section, it is generally porphyritic and hypocrySTALLINE, and exhibits ophitic texture and, at places, intergranular, sub-ophitic and variolitic. Phenocrysts are pre-dominantly plagioclase, with minor olivine and pyroxene and opaque minerals. Spherulite structures are also identified in a highly altered sample from the contact zone between basalt and serpentinite in a quarry, near Corbyn's Cove in South Andaman. This sample is a hybrid one with a relict basalt portion exhibiting typical intergranular texture, being invaded by serpentinous material, and later by a quartz vein (Fig 5.1f). The spherulites found in Andaman Island represent altered glassy groundmass.

Plagiogranites are fine to coarse grained leucocratic rocks composed mainly of plagioclase and quartz with minor amount of amphibole and biotite. Plagiogranites of the sequence represent the end product of sub-alkaline tholeiitic magmatism. These plagiogranites are associated with cumulates, suggesting their formation either by crystal-liquid fractionation process (Coleman and Peterman, 1975) or by late stage silicate liquid immiscibility process (Dixon and Rutherford, 1979). In thin section, plagiogranites are medium to coarse grained, almost equigranular and subhedral in shape recognized as hypidiomorphic granular texture (Fig 5.1a). Apart from this, poikilitic and granophyric

textures are also observed, in which laths of plagioclase feldspars are enclosed by big quartz crystals and have intergrowths of quartz and plagioclase feldspar, respectively.

6.1.2 Inferences from geochemistry

Based on major oxide we have observed three compositionally different units in the Andaman Ophiolite Group. The first group has lower silica (39-44%), high TiO_2 (1-1.5%) and low alumina (10-14%), the second group contains low silica (45-50%), moderate TiO_2 (0.7-1%) and high alumina (15-19%) and third group has high silica (more than 60%) low TiO_2 (0.5%), moderate alumina (10-13%) and low MgO (~2%). We made an attempt to classify some of these rocks, using their total alkalis (TA) and silica (S) contents (Le bas et al., 1986), which were seemed to be unaltered or least altered based on petrography. Figure 6.1 shows the results of this classification. In the figure, the data are plotted according to the type of emplacement of the rock: a) volcanic (basalts) b) plutonic (gabbro, pyroxenite etc.) and c) intrusive (plagiogranites). The volcanic rocks have wide variations in silica (42-51%) as well as in alkali (0.2-4.1%) as compared with plutonic rocks in which silica varies from 45 to 47% and alkali from 0.9 to 2.5%. From TAS plot it is evident that plutonic rocks are basaltic where as volcanic rocks are picobasaltic to basaltic in composition. Plagiogranites have high silica (~ 63-78%) with low K_2O (0.02-0.04%), high Na_2O (1.67-5.2%) and high P_2O_5 (0.2-0.3%) contents as compared with volcanic and plutonic rocks. In the TAS diagram (Fig. 6.1), plagiogranites fall in dacitic and rhyolitic fields.

A majority of rock units from the ophiolite sequence are highly altered, which is evident from presence of alteration products (e.g., serpentine) and high LOI %, that varies from ~ 3 -10 %. Niu (2004) showed that sea floor weathering is responsible for loss of MgO . Some of the

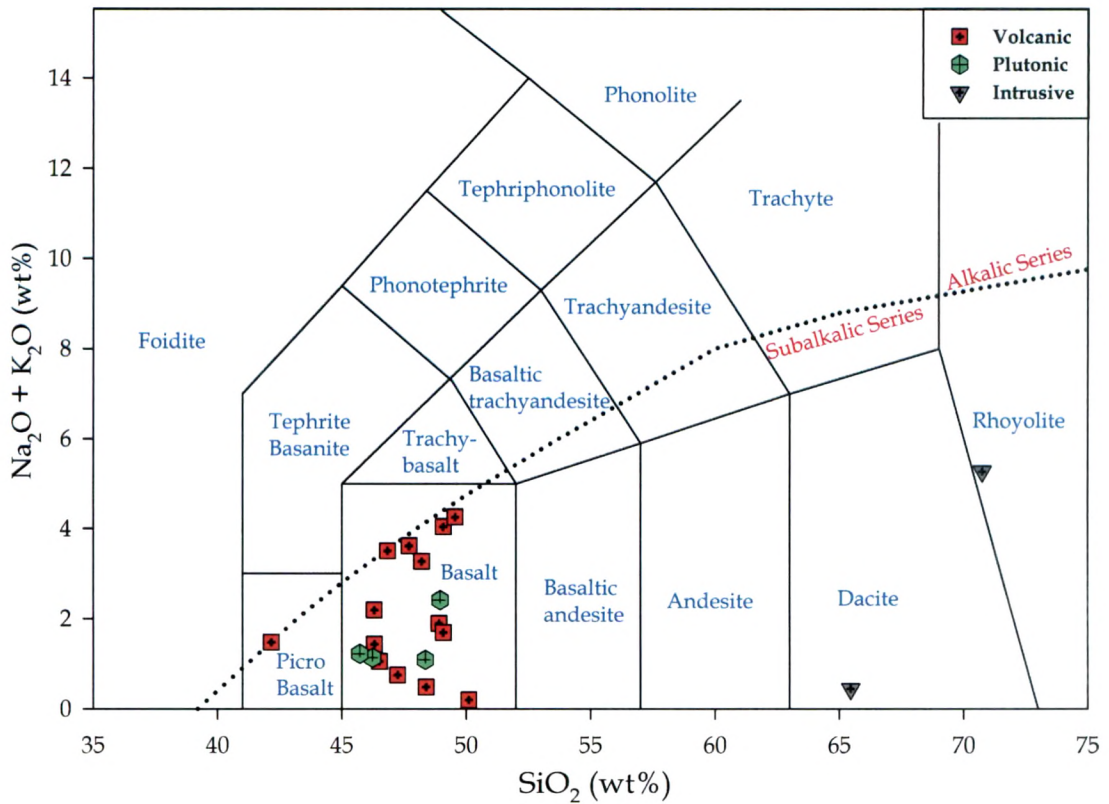


Fig. 6.1 Classification of Andaman Ophiolites based on Total Alkali vs. Silica variation (after La Bas et al; 1986). The dashed line marks the boundary between alkalic and subalkalic series (Irvine and Baragar, 1971).

ophiolite samples show low silica and low MgO contents that probably suggest sea floor weathering. The SiO_2/MgO vs. Al_2O_3 variations in least altered ophiolite samples overlap with the field for Oman ophiolites (Fig. 6.2). This suggests that both ophiolites had similar petrogenetic histories.

The variation of TiO_2 versus MgO in Andaman Ophiolites (Fig. 6.3) suggests that these rocks are created from polygenetic melt with high MgO and low TiO_2 and low MgO and high TiO_2 . The high MgO and low TiO_2 with high Cr contents suggest that these rocks belong to suprasubduction zone forearc ophiolites (Dilek and Furnes, 2011) that show invariably low TiO_2 and high Cr contents. The rock with low MgO and high TiO_2 possibly represent volcanic arc type ophiolites (Dilek and

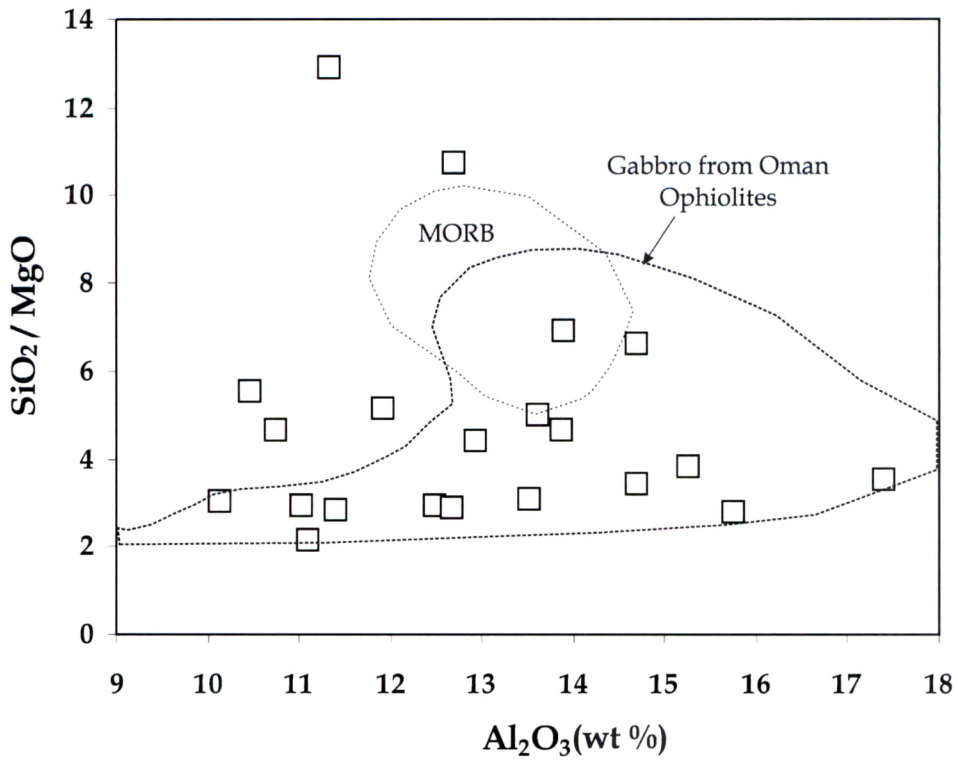


Fig. 6.2 SiO_2/MgO vs. Al_2O_3 plot for Andaman Ophiolites. Also shown are fields for Oman Ophiolites and MORB. Data sources: Oman ophiolites: Khotin and Shapiro (2006); MORB: Rollinson, (1993).

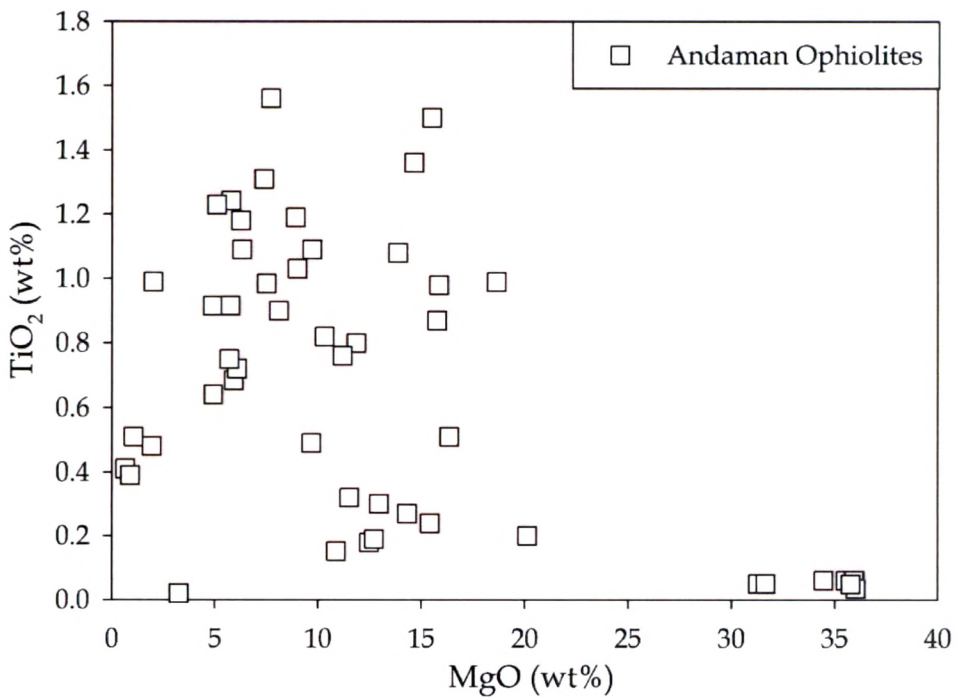


Fig. 6.3 MgO vs. TiO_2 variation plot for rocks from the Ophiolite Group

Furnes, 2011). Thus it appears that the ophiolites of Andaman, although have a predominant suprasubduction zone origin, may also contain some rocks with arc affinity.

Chondrite normalized REE patterns for rocks from Ophiolite Group overlap with those of the rocks from Oman Ophiolites of similar origin (Fig. 6.4). Interestingly, some of the basalts have MORB like patterns, which possibly hints at the fact that the mantle at the subduction zone during the initiation process was a MORB source type of mantle, i.e. depleted in LILE. Plagiogranites show LREE enriched patterns, typical of suprasubduction zone ophiolites (e.g., Pearce et al., 1984).

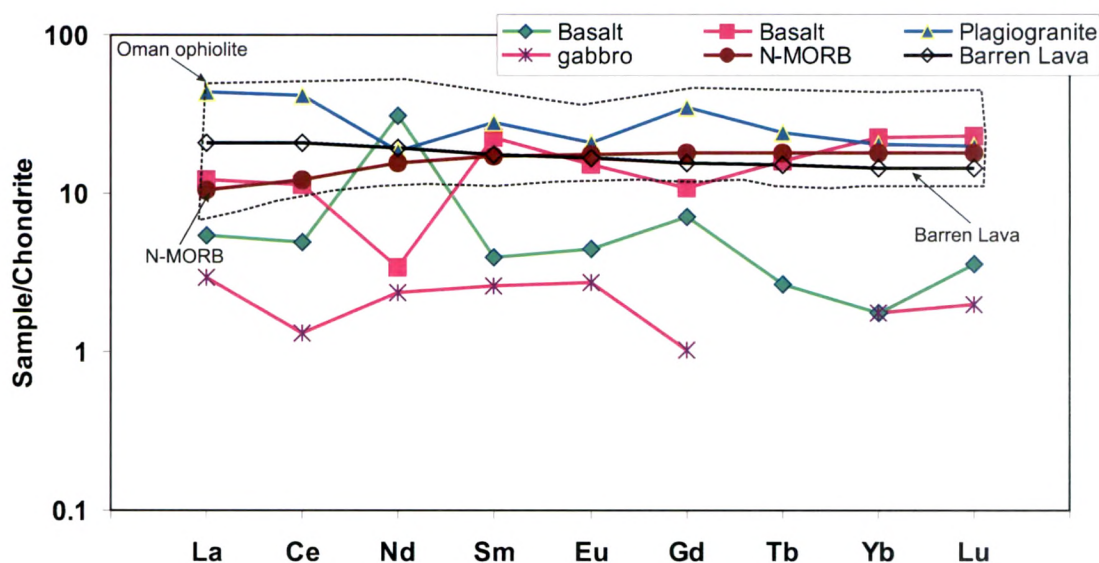


Fig. 6.4 Chondrite normalized REE patterns for rocks from the Ophiolite Group. N-MORB (Sun and McDonough, 1989), Barren Island lavas and Oman ophiolite field (Godard et al., 2003) are plotted for comparison.

The Ti versus V discrimination diagram has been very useful in understanding the provenance and the tectonic environments of ophiolites suite of rocks (Shervais, 1982). In such a plot (Fig. 6.5) the rocks from the Ophiolite Group appear to suggest that they may not have been derived from a single melt source. One set of data, which have low Ti and low V,

fall in the boninite field. The second set having high alumina, low Ti and low Ti/V are typical of arc volcanics. The third set having Ti/V ratios of 20 - 30 have mixed signatures of mid oceanic ridge basalt and island arc volcanics.

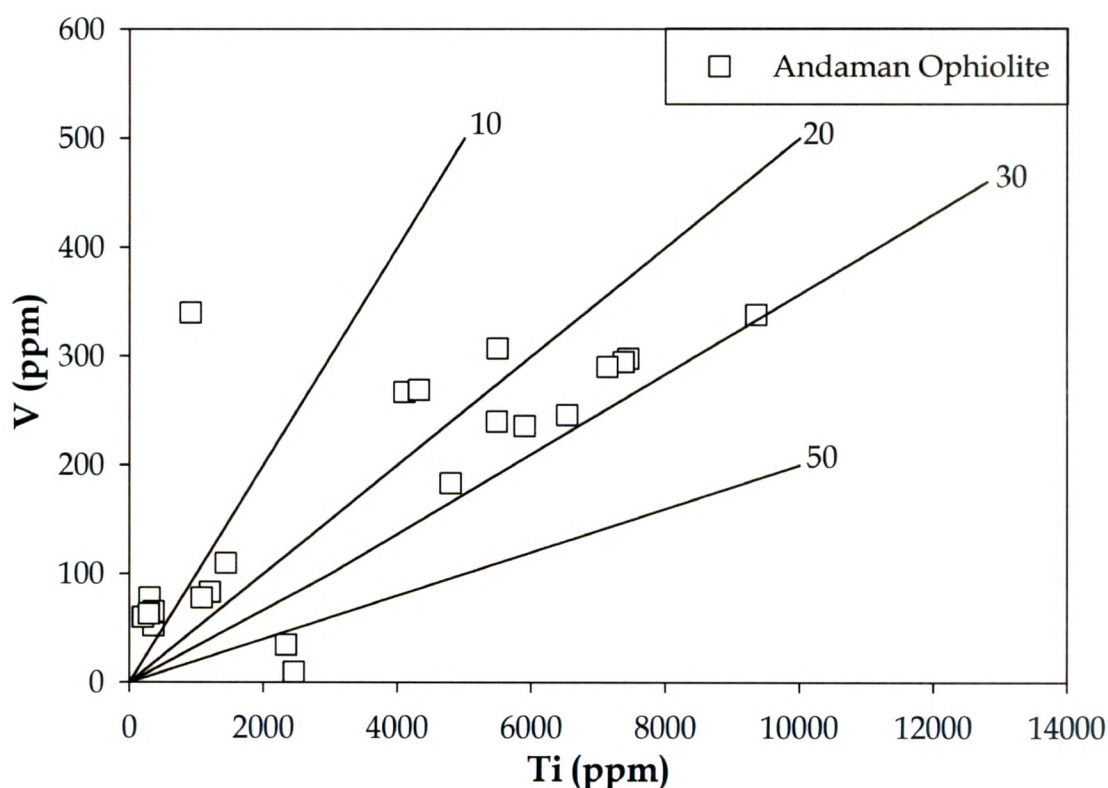


Fig. 6.5 Ti - V discrimination plot for rocks from the Ophiolite Group

The radiogenic isotopic ratios of Nd and Sr have also been used to decipher source compositions of the ophiolites and the effects of subduction zone components on their chemistry. However, our inferences are of limited in nature due to lack of sufficient data on these rocks. Figure 6.6 and 6.7 utilize Sr-Nd isotopic ratios and SiO₂ variations in these rocks to understand their petrogenesis. Isotopic ratios used are initial ratios, corrected for radiogenic growth assuming as age of 100 Ma (e.g., Pederson et al., 2010). In Fig. 6.7, we compare our data with those from the Oman ophiolites.

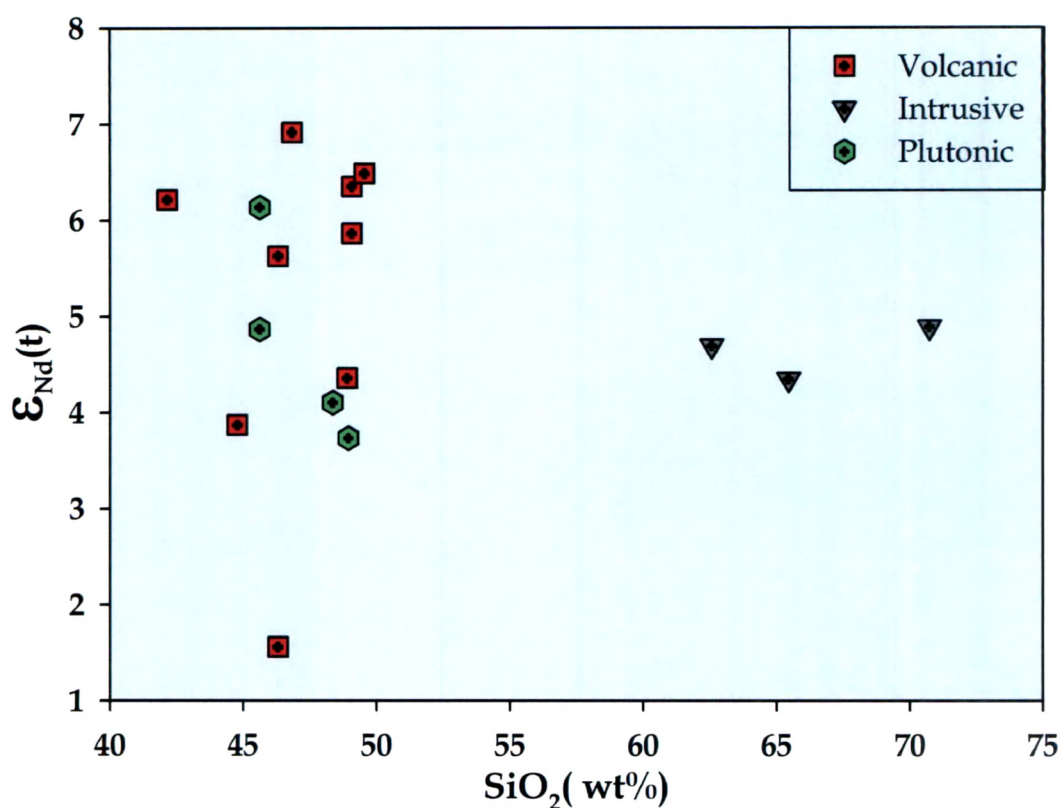


Fig. 6.6 $\epsilon_{Nd}(t)$ versus SiO_2 plot for rocks from Ophiolite Group.

As can be seen from Fig. 6.6, the volcanic and plutonic units of the ophiolites show a large spread in $\epsilon_{Nd}(t)$ within a small range of SiO_2 , whereas the intrusive plagiogranites have constant $\epsilon_{Nd}(t)$ for a large spread in SiO_2 . The $\epsilon_{Nd}(t)$ variation in the former units clearly points to the possibility that at least two end-members were involved in the generation of magmas for these rocks - one with high ϵ_{Nd} and other with lower ϵ_{Nd} . The former is obviously a MORB mantle and the later could have been the influence of fluids and/or sediments derived from slab. The evidence that subduction component is present in these rocks, clearly indicates that the Andaman ophiolites are, at least partly, of suprasubduction zone origin.

In the plot of $^{143}Nd/^{144}Nd(t)$ versus $^{87}Sr/^{86}Sr(t)$ the rocks of Andaman ophiolites show identical Nd isotopic ratios to that of Oman

ophiolites and volcanics from the Andaman arc (e.g., Barren Island), however have intermediate Sr isotopic ratios (Fig. 6.7). These observations very clearly confirms our earlier observations that the ophiolites in the Andaman subduction zone have sampled a source that started as a depleted MORB type mantle and later on got enriched through fluids and/or sediments derived from the subducting slab. It also appears that the Andaman ophiolites formed during a prolonged magmatic event and that may be the reason why they have sampled the evolving source so as to have all two distinct ophiolites: MORB - type and volcanic arc type.

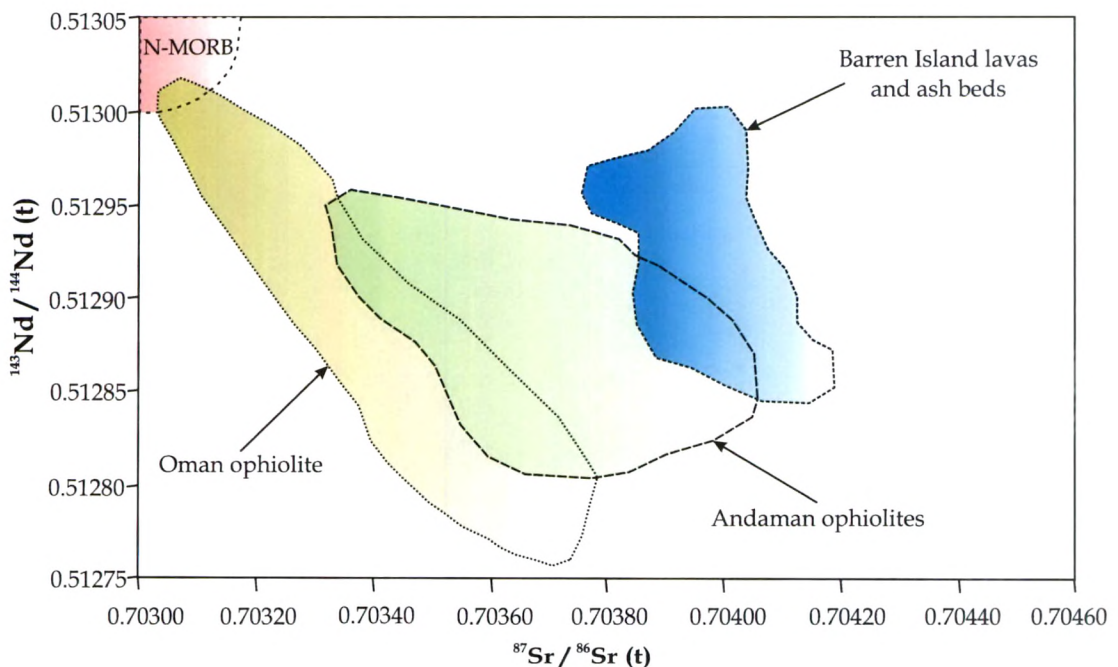


Fig. 6.7 $^{143}\text{Nd}/^{144}\text{Nd}(t)$ vs. $^{87}\text{Sr}/^{86}\text{Sr}(t)$ for Andaman ophiolites, compared with the fields for MORB, Oman ophiolites and Barren Island lava flows (Data source: Oman ophiolites field: Amari et al., 2007 and N-MORB: Rollinson, 1993).

6.2 Origin of Andaman mud volcanoes

6.2.1 Morphology

Mud volcanoes of the Andaman Islands are located along the N-S trending faults. Water, light grey coloured clay (mud breccias), gas and hydrocarbons are continuously expelled from these mud volcanoes

forming large mud mounds inside dense forest. These mud mounds are dome shaped structures rising about 25 -30 m above present sea level (Fig. 2.5). The crests of the domes are nearly one meter in height and have circular craters of about 0.2 to 0.3 m across. The gases emitted are

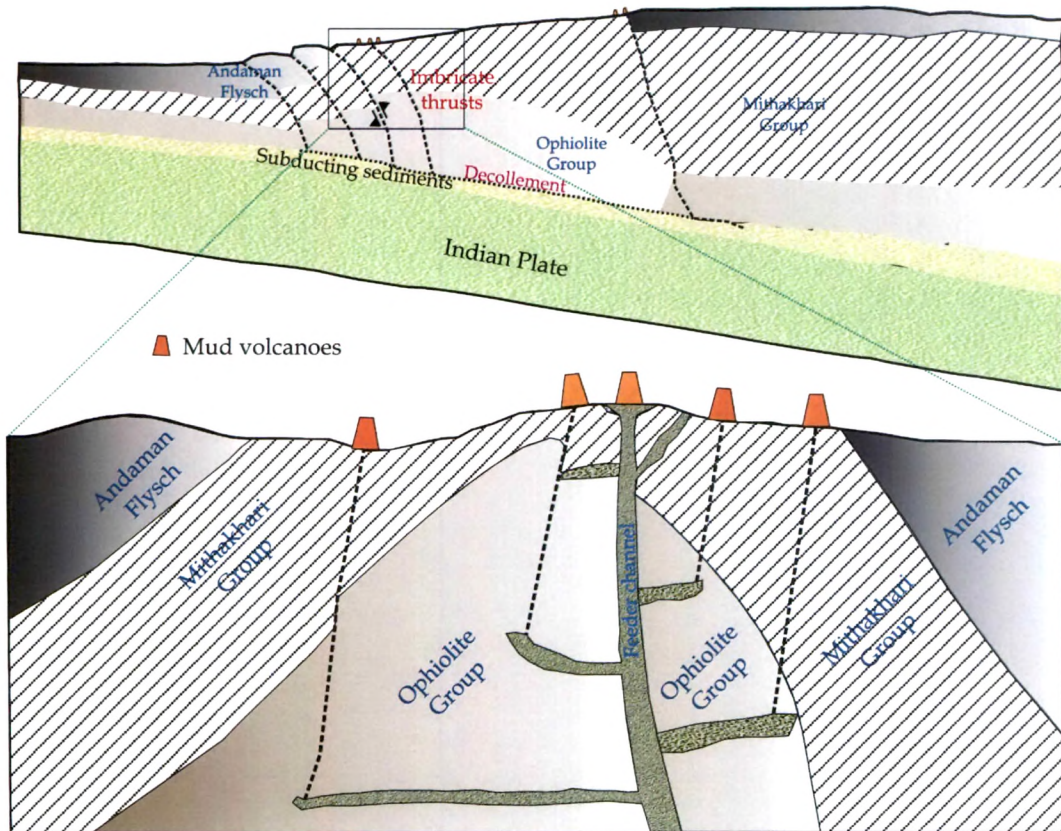


Fig. 6.8 Schematic cross-section showing lithostatic units and the origin of mud volcanoes of Andaman Islands based on author's interpretations. (b) is an enlarged portioned of the box shown in (a).

dominated by methane confirmed by their ability to catch fire. According to local people, the gas emission activity increases during earthquakes, which confirms that the mud volcanoes are linked to the underground fault systems. The rock clasts and mud breccias that are ejected from mud volcanoes are pillow lavas and sediments from the underlying sedimentary formations (Fig. 6.8). In the field, it was observed that the

mud volcanoes of south Andaman are more active as compared with mud volcanoes of middle Andaman. Based on our field observations we proposed morphology for a mud volcano plumbing system as shown in Fig. 6.8. According to this model, a mud volcano field is fed by a major feeder channel that originates from the boundary between the subducting and overriding plates and numerous secondary or distributory channels (Fig. 6.8).

6.2.2 Clay mineralogy of mud breccia

A total number of 20 samples of mud breccias were analyzed for their clay mineralogy by X-Ray powder diffraction method. The diffractograms are presented in Fig. 5.3 and Fig. 5.4. These results suggest that the mud breccias of Andaman mud volcanoes are made up predominantly of kaolinite, chlorite and smectite (Fig. 5.3). Albite and small amount of muscovite also appear to be present. A small amount of calcite present in Baratang mud breccias. The above mineralogical compositions suggest that the mud breccias are derived mostly from mafic rocks through alteration, and that these mafic rocks are presumably the rocks of the slab that have undergone extensive alteration in the sea. However, we cannot rule out the presence of clay minerals derived from the subducting sediments and/or overlying Andaman rocks through which the mud volcanoes have erupted.

6.2.3 Stable isotopic compositions of mud water

Understanding the source and origin of the water in mud volcanoes is an active field of research, because these are believed to represent fluids of the subduction zone and thereby can shed light on subduction zone processes within the accretionary wedge. At depth in the accretionary wedge, fluid-sediment interactions affect the chemistry of fluids and their distinct signatures are brought to the surface by the ascending mud

volcano fluids. However, surface processes such as mixing with ground water or rain and interaction with host rocks can also affect the chemistry of the fluids. Therefore, to trace the origin of mud volcano fluids we have utilized stable O and H isotopic variations in them. These data are presented in Table 5.5 and plotted in Fig. 6.9.

$\delta^{18}\text{O}$ and δD of the water samples of mud volcanoes of Baratang (middle Andaman) and Diglipur (north Andaman) range from -0.2‰ to 2.6‰ and -13.6‰ to -26.3‰ with respect to V-SMOW, respectively (Fig. 6.9a). These values suggest that these waters are neither derived from sea water nor from meteoric water. As can be seen in fig 6.9a, the isotopic compositions of mud waters are very different from those of local groundwater, local fresh water springs and seawater. From Fig. 6.9b it is also clear that these waters are not produced by mixing of these three end members as they plot far away from meteoric water line. The $^{87}\text{Sr}/^{86}\text{Sr}$ of these waters (average = 0.707) also rules out the possibility that these are pure present day seawater – for which the value is 0.7092.

In $\delta^{18}\text{O}$ vs. δD plot (Fig. 6.9a) the mud waters from both mud volcanoes show linear trends starting from compositions with lower values. Such trends are typical of evaporation and/or mixing with end members having higher $\delta^{18}\text{O}$ and δD . The possibility of later is ruled out as such end members do not appear to exist in the Andaman Islands. To simulate the observed linear variations by evaporation process we modelled the data using a simple Rayleigh fractionation process. The single component Rayleigh equation (Rayleigh, 1896, Ray and Ramesh, 2000) for evaporation of water body can be written as:

$$\delta_{\text{water}} = (\delta_{\text{water}}^{\text{initial}} + 10^3) f^{(\alpha-1)} - 10^3 \quad (6.1)$$

Where $\delta_{water} = \delta^{18}\text{O}$ or δD of the water body at anytime

$\delta_{water}^{initial} = \delta^{18}\text{O}$ or δD of the water body at time, $t = 0$

f = fraction of remaining water (reservoir)

α = temperature dependent equilibrium fractionation
factor for H or O between vapour and water

The average ambient temperature at the sites of these mud volcanoes is measured to be 32°C, which is taken as the temperature of evaporation and α for O and H are determined from the relationships given by Harita and Wesolowski (1994) and Kakiuchi and Matsuo (1979), respectively. Assuming initial isotopic compositions of the water to be: $\delta^{18}\text{O} = 1.0\text{‰}$ and $\delta\text{D} = -27.5\text{‰}$, we could explain the trend shown by the mud water samples from diglipur by equation 6.1 (Fig. 6.9a) with a maximum amount of evaporation of 10%. The samples from mud volcanoes of Baratang also show similar evaporation trend, however, their starting compositions appear to be different, which clearly is a result of mixing with local ground water (Fig. 6.9a). Mixing calculations suggest that the initial isotopic compositions of Baratang mud waters could have been identical to those from Diglipur, however mixing of up to 30% of local ground water ($\delta^{18}\text{O} = -2.21\text{‰}$, $\delta\text{D} = -10.60\text{‰}$) changed them prior to their further fractionation by evaporative processes. We, therefore, conclude that the representative non-fractionated isotopic compositions of waters from mud volcanoes of Andaman are: $\delta^{18}\text{O} = 1.0\text{‰}$ and $\delta\text{D} = -27.5\text{‰}$ with respect to V-SMOW.

As mentioned earlier, the mud waters of Andaman Islands do not appear to have been derived from fresh waters of the region since their isotopic compositions are far below the global meteoric water line (Fig. 6.9b). They also do not represent the seawater. However considering their

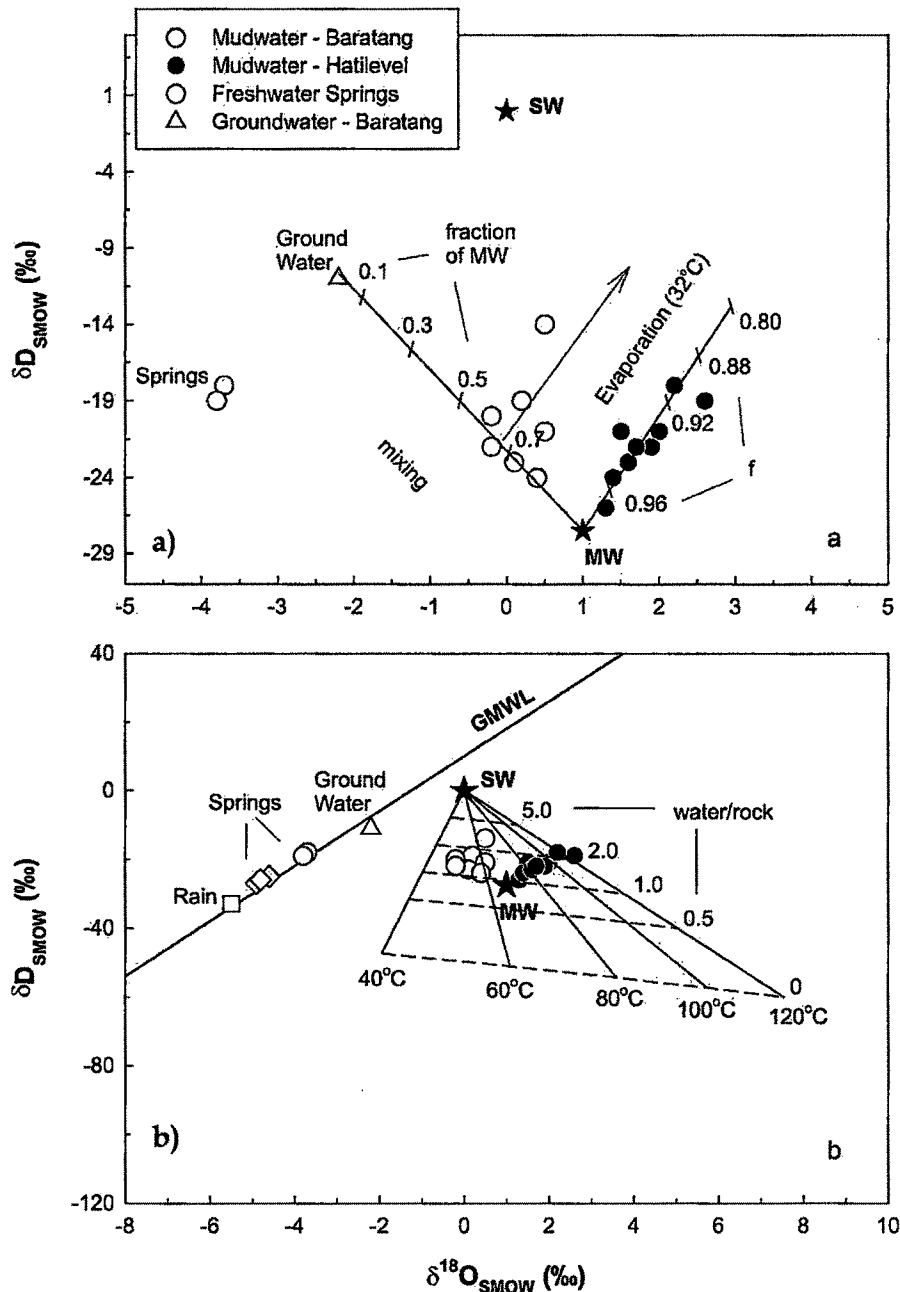


Fig.6.9 $\delta^{18}\text{O}$ and δD plots for water samples from mud volcanoes and fresh water sources of Andaman Islands (a) the data for North Andaman (Hathilevel, Diglipur) are explained by evaporation (Rayleigh fractionation) at 32°C, whereas those for middle Andaman (Baratang) are explained by binary mixing with ground water and subsequent evaporation. MW = starting compositions for mud water; f = fraction of remaining reservoir during evaporation; SW = Sea Water. (b) The solid lines are evolutionary paths at different temperatures in a water-rock interaction model, where the initial water is seawater (SW) and initial rock/mineral is a smectite clay ($\delta^{18}\text{D} = -85\text{‰}$; $\delta^{18}\text{O} = 20\text{‰}$). The dashed lines join water compositions at a particular water/rock during the evolutions. GMWL = Global Meteoric Water Line.

salty taste and closeness of their $\delta^{18}\text{O}$ to that of the seawater we envisage that the mud waters are modified seawater. As we know mud waters accompany clay minerals (mud breccia) and come from a greater depth within the accretionary wedge, therefore, it is highly likely that the water released from clay minerals due to dehydration processes might have freshened the seawater that accompanied them. In other words, the seawater that accompanied the subducting sediments had its isotopic compositions modified due to interaction with the dehydrating clay minerals at highly compressive regimes of the accretionary prism. To test this hypothesis we took help of a water-rock interaction model developed by Ray and Ramesh (1999) - the details of which are presented below.

In the water-rock interaction model of Ray and Ramesh (1999), isotopic exchange of hydrogen and oxygen can be written as the following two simple mass balance equations:

$$W_H \delta D_{\text{water}}^i + R_H \delta D_{\text{rock}}^i = W_H \delta D_{\text{water}}^f + R_H \delta D_{\text{rock}}^f \quad (6.2)$$

$$W_O \delta^{18}\text{O}_{\text{water}}^i + R_O \delta^{18}\text{O}_{\text{rock}}^i = W_O \delta^{18}\text{O}_{\text{water}}^f + R_O \delta^{18}\text{O}_{\text{rock}}^f \quad (6.3)$$

Where ' W_H ' and ' W_O ' are amounts of hydrogen and oxygen respectively, in the water expressed in moles. ' R_H ' and ' R_O ' are those for the rock. Superscripts 'i' and 'f' stand for initial and final compositions, respectively. From these two equations final rock compositions can be determined. The relations for the final rock compositions are:

$$\delta D_{\text{rock}}^f = \frac{\left(\frac{W_H}{R_H}\right) \delta D_{\text{water}}^i - \Delta_{\text{rock-water}}^H + \delta D_{\text{rock}}^i}{1 + \left(\frac{W_H}{R_H}\right)} \quad (6.4)$$

$$\delta^{18}O_{rock}^f = \frac{\left(\frac{W_o}{R_o}\right) \delta^{18}O_{water}^i - \Delta_{rock-water}^O + \delta^{18}O_{rock}^i}{1 + \left(\frac{W_o}{R_o}\right)} \quad (6.5)$$

Where $\Delta_{rock-water}^H$ and $\Delta_{rock-water}^O$ stand for the differences between final isotopic compositions of the rock and fluid (for hydrogen and oxygen, respectively). These are also respectively the equilibrium hydrogen and oxygen isotopic fractionation factors between the rock and water ($10^3 \ln \alpha_{rock-water}$), expressed in per mil (‰) units. Considering that both the water and rock reservoirs are very large, the water-rock ratios for both H and O can be considered identical, i.e., $\frac{W_H}{R_H} = \frac{W_O}{R_O}$.

In the present situation our rock is made up of clay minerals, predominantly smectite. Therefore we utilized temperature dependant fraction factors for smectite-water from Sheppard and Gilg (1996) and Yeh (1980) and generated model curves using equations 6.4 and 6.5 at temperatures ranging from 40° - 120°C and W/R ratio varying from 0 to infinity (Fig. 6.9b). Comparison of model curves with the data for mud water reveals that the observed unfractionated isotopic compositions of these waters can be easily explained by clay-seawater interaction at a temperature of ~ 70°C and W/R of 1.0. Clearly the original mud water appears to be of seawater composition that got modified due to interaction with dehydrating clays in the subduction environment. In summary, the mud waters of Andaman Islands are originally derived from seawater trapped in the slab-sediments.

6.2.4 Origin of mud breccias

Mud breccia constitutes the solid portion of the materials that ooze out of mud volcanoes. It consists of a clay matrix (Fig. 5.4) with minor carbonate and plenty of pebble to boulder size rock clasts. The rock clasts are clearly derived from the overlying sedimentary formations through which the mud volcanoes of the Andamans have erupted. The minor carbonates are mostly composed of foraminiferal tests that too appear to have been derived from fossiliferous carbonate formations present within the Mithakhari and Andaman Flysch Groups. It is the mud matrix, the main component of the breccia that holds keys to our understanding of the origin of these mud volcanoes and processes that occur within the accretionary wedge. In the following section we discuss our findings from the geochemistry of mud matrix and attempt to decipher their origin.

Clues from major and trace elements

The major oxide data for mud breccia samples are given in Table 5.1a and are plotted in the chemical classification diagram of Herron (1988), which is extensively used for geochemical classification of mudstone and sandstone (Fig. 6.10). It is observed that most of the mud breccias from Baratang and Diglipur fall on the boundary between shale and Fe-shale suggesting that the mud matrix in these samples is derived from deeper level (in deep water regime) and has little influence of surface weathering. Samples of mud breccia and serpentinite clasts (that appear to be highly weathered and possibly represent the source of the mud breccia) are plotted on the A-CN-K ($\text{Al}_2\text{O}_3\text{-CaO}^*\text{+Na}_2\text{O-K}_2\text{O}$) diagram of Nesbitt and Young (1984) in Fig. 6.11, in which the oxide are represented in molar proportions and the CaO^* represents the carbonate free CaO. Samples from Andaman Ophiolite Group are also plotted in the diagram that roughly resembles the slab basalts (oceanic crust). As can be seen from the plot, the mud breccias show a trend at a low angle to the A-CN join,

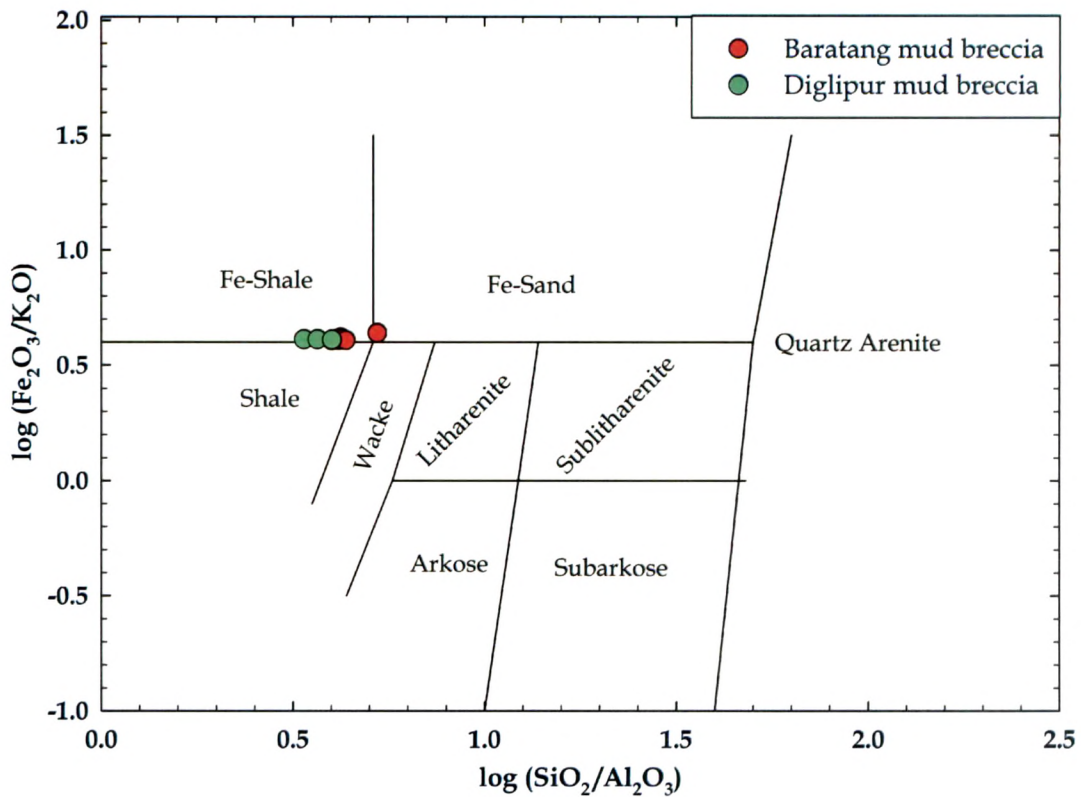


Fig. 6.10 Chemical classification of mud breccia from the mud volcanoes of Andaman, using the scheme of Herron (1988)

starting from pyroxenite compositions to smectite \pm illite compositions through altered basalt (or serpentinite). Clearly the major contributors of the clay minerals of mud breccia are mafic rocks and in our case the altered oceanic crust of the slab.

We have plotted variation diagrams (Fig. 6.12) for all the major oxides that represent purely the mud matrix (not the water) with respect to 'Al', since 'Al' is a true representative of the clay minerals present in the mud matrix. The linear relationships shown by SiO_2 with Al_2O_3 (Fig. 6.12a) rules out the possibility of presence of any other mineral - other than alkali-alumino-silicates in most of the breccia samples. This inference is supported by the low CaO contents and its no apparent correlation with Al_2O_3 (Fig. 6.12c). Positive correlation between K_2O with Al_2O_3 suggests

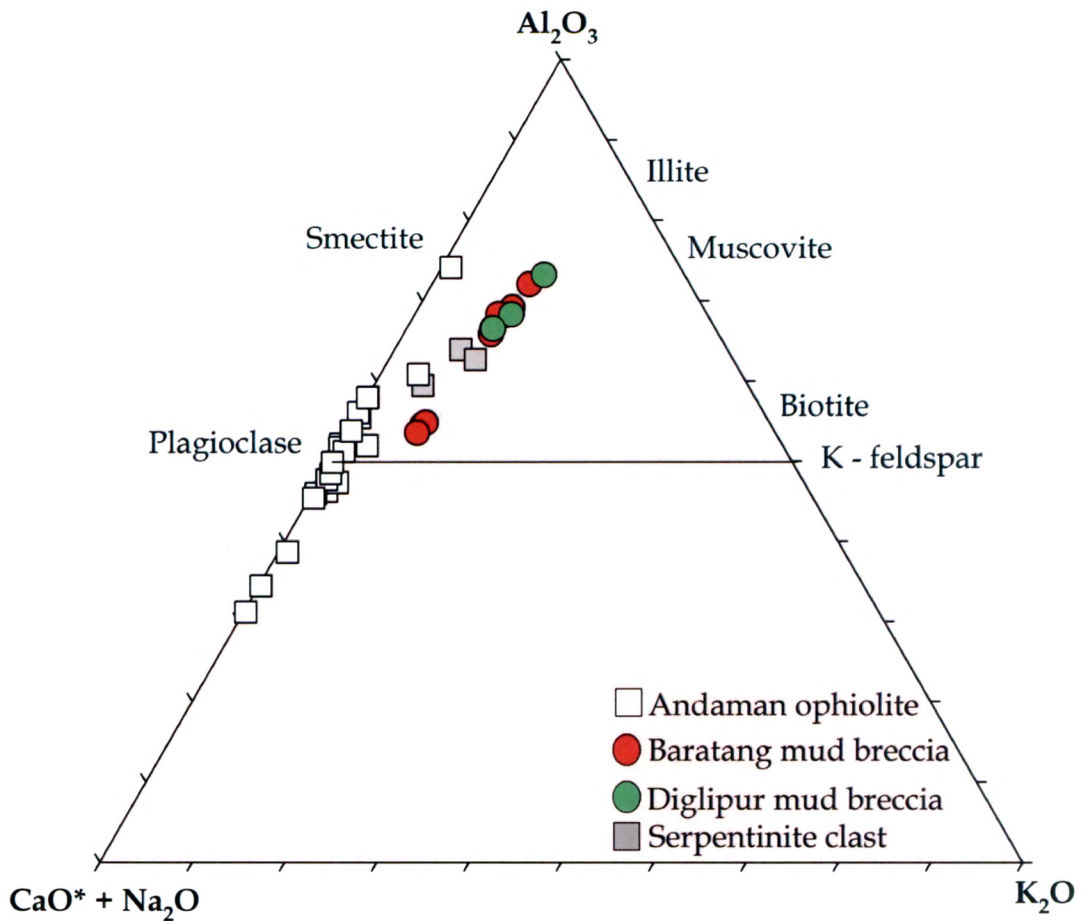


Fig. 6.11 Mud breccias and serpentine clasts from mud volcanoes of Andaman Islands are plotted on A-CN-K diagram of Nesbitt and young (1984). Also plotted are the rocks of the Andaman Ophiolites.

the presence of illite as the predominant clay, which did not get reflected in our simple powder diffraction X-Ray analyses. Proper identification of individual clays would require glycolation and heating. High MgO and TiO_2 hint at the possibility that clays derived from basaltic rocks dominate the matrix.

Concentration variations in trace elements have been useful in understanding provenance, weathering and transportation. The Rare Earth Elements (REEs) patterns have been exclusively used in deciphering

history of the sediments especially mud and mud stones (shale). The REEs, due to their group behaviour, immobility in water, and almost nonexistent inter element fractionation; faithfully preserve the source compositions (McLennan et al., 1989).

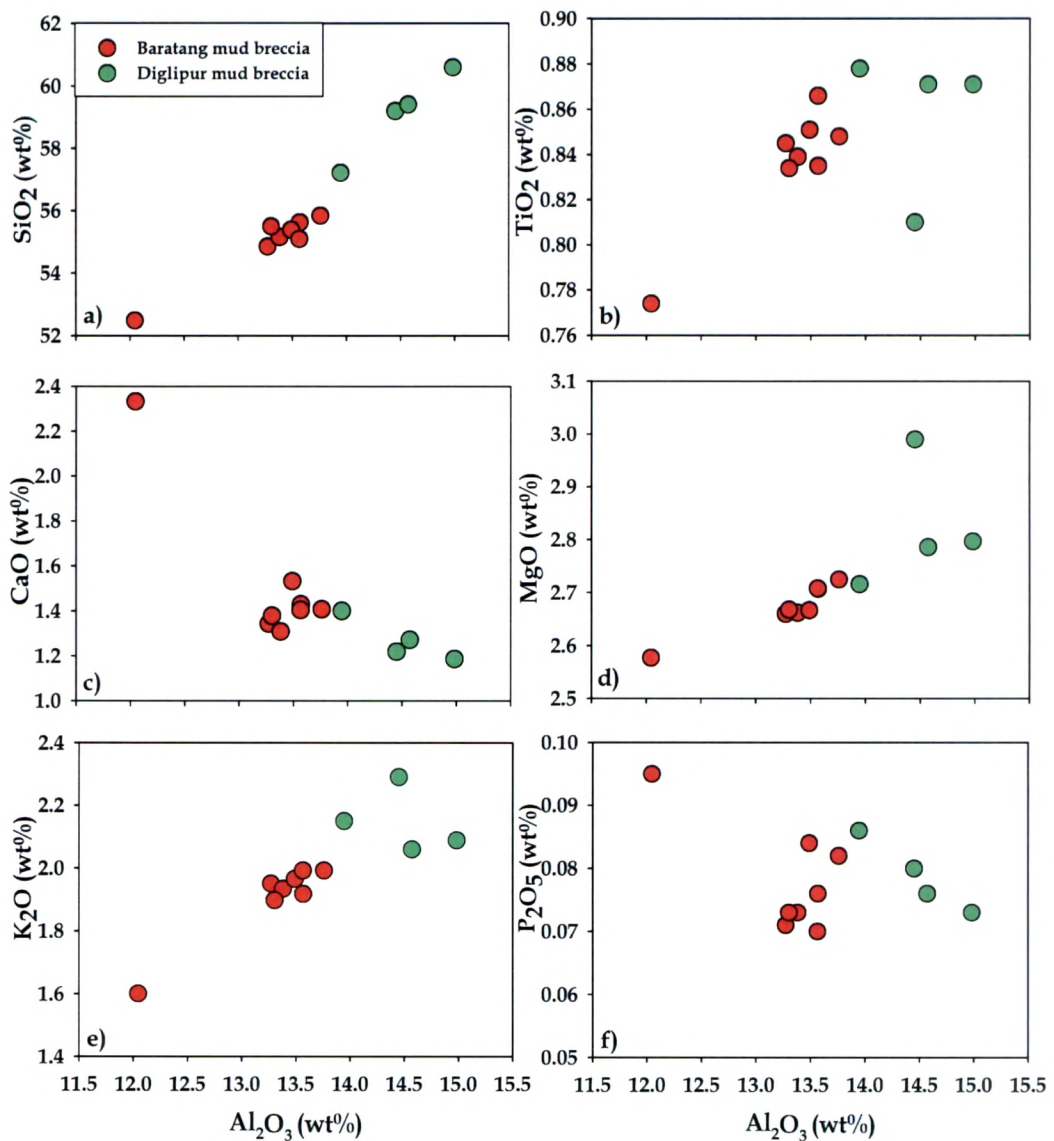


Fig. 6.12 Major element variation diagrams for mud breccias from the mud volcanoes of Andaman Islands

Chondrite normalized REE patterns of mud breccia and serpentinite clasts from mud volcanoes of Andaman islands along with

PAAS and Indian Ocean sediments (siliceous ooze, calcareous ooze and red clay; Pattan et al., 1995) are plotted for comparison in Fig 6.13. The REE patterns of mud breccia are very different from that of the red clay and calcareous ooze, but overlap with those of the serpentinite clasts, PAAS and siliceous ooze. Therefore, we are inclined to believe that the clay minerals in mud matrix represent alteration products of oceanic crust and terrigenous sediments and have very little contribution from pelagic sediments. The same can be interpreted from the multi element variation diagram in Fig. 6.14. As can be seen in this N-MORB normalized plot the trace element patterns for the mud breccia samples can be explained if their source had been the 'altered oceanic crust' as represented by the serpentinite clasts.

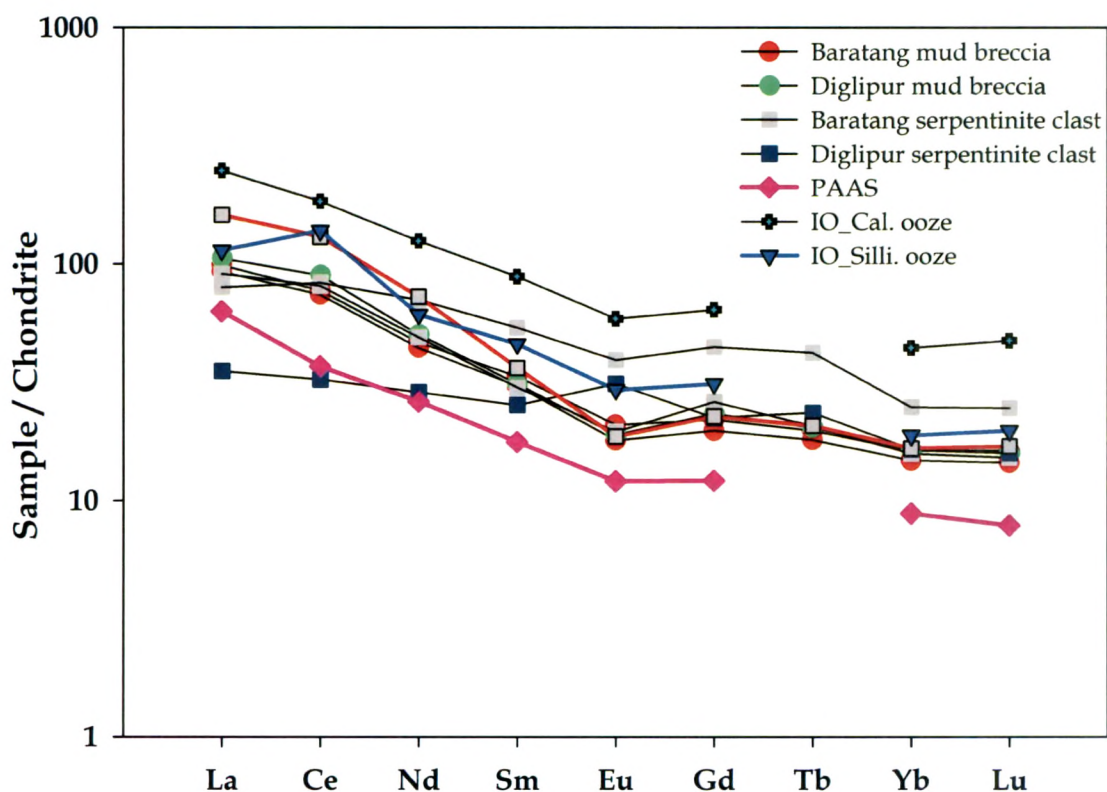


Fig.6.13 Chondrite normalized REE patterns for mud breccia and serpentinite clasts compared with PAAS (McLennan et al., 1989) and Indian Ocean sediments (Pattan et al., 1995)

Interestingly, many of the important features observed in the trace element patterns (N-MORB normalized) of arc lavas such as: 1) Ta depletion, 2) P depletion, 3) Ti depletion, and 4) K enrichment; are also observed in mud breccia (Fig. 6.14). Since mud breccia is derived from very deep part of the accretionary wedge, possibly from the slab-wedge interface, and represents the sediments of the slab that are transported into the mantle, we are inclined to believe that all the above geochemical features observed in arc lavas are contributed by the slab sediments through mud breccia, whereas other features such as enrichment in Ba in arc lavas is a result of Ba mobilization through fluids into the mantle wedge, as a result mud breccia representing the slab sediments becomes depleted in it.

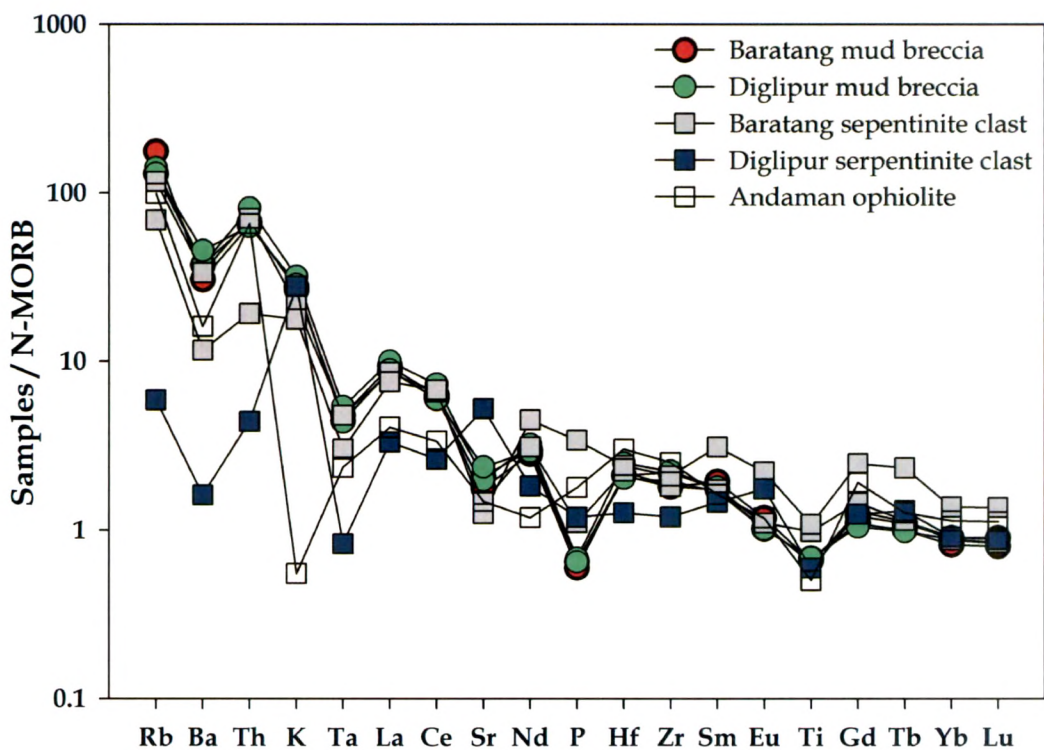


Fig.6.14 N-MORB normalized (Sun and McDonough 1989) trace element patterns of mud breccias, serpentinite rock clasts compared with the pattern of Andaman Ophiolite

Carbon and Nitrogen abundance of the mud breccia samples of mud volcanoes of Baratang (middle Andaman) and Diglipur (north Andaman) range from 0.5 to 0.9 and 0.6 to 0.12, respectively (Table 5.4). Lower abundances of carbon and nitrogen in mud breccia suggest that these are derived mainly from hemipelagic sediments. Low C/N ratios may indicate microbial activity in the sediments (Berner, 2006).

Clues from radiogenic isotopes

To further understand the source and origin of mud breccia we took the help of radiogenic Sr and Nd isotopic ratios as tracers (using data presented in Table 5.3a). The data are plotted in a $\epsilon_{Nd}(0)$ versus $^{87}Sr/^{86}Sr$ diagram in Fig. 6.15 along with data for 2N HCl leached mud breccia samples, serpentinite clasts and samples from Andaman ophiolites. These data are compared with fields of fresh Indian Mid Oceanic Ridge Basalts (I-MORB), altered I-MORB and sediments from Bay of Bengal (BOB). It is observed that the mud breccia samples have $^{87}Sr/^{86}Sr$ close to 0.7092, which is same as the isotopic composition of the present day seawater. Since these samples were not washed to remove the mud-water from it the isotopic composition is a mixture of that of the pure solid silicate mud and mud water. As water is an integral part of the subducting materials it's isotopic composition cannot be ignored from the discussion. Therefore, that the Andaman slab sediments represented by the mud breccia, have $^{87}Sr/^{86}Sr$ and $\epsilon_{Nd}(0)$ isotopic compositions in the range of 0.70854 to 0.70986 and -3.4 to -1.7, respectively. Interestingly, the mud water that accompanies the breccia has $^{87}Sr/^{86}Sr$ ratio of 0.707, which is different from the present-day seawater and pure silicate fraction of the breccia has values > 0.711 . This suggests that the isotopic compositions of the mud water are not influenced by the breccia.

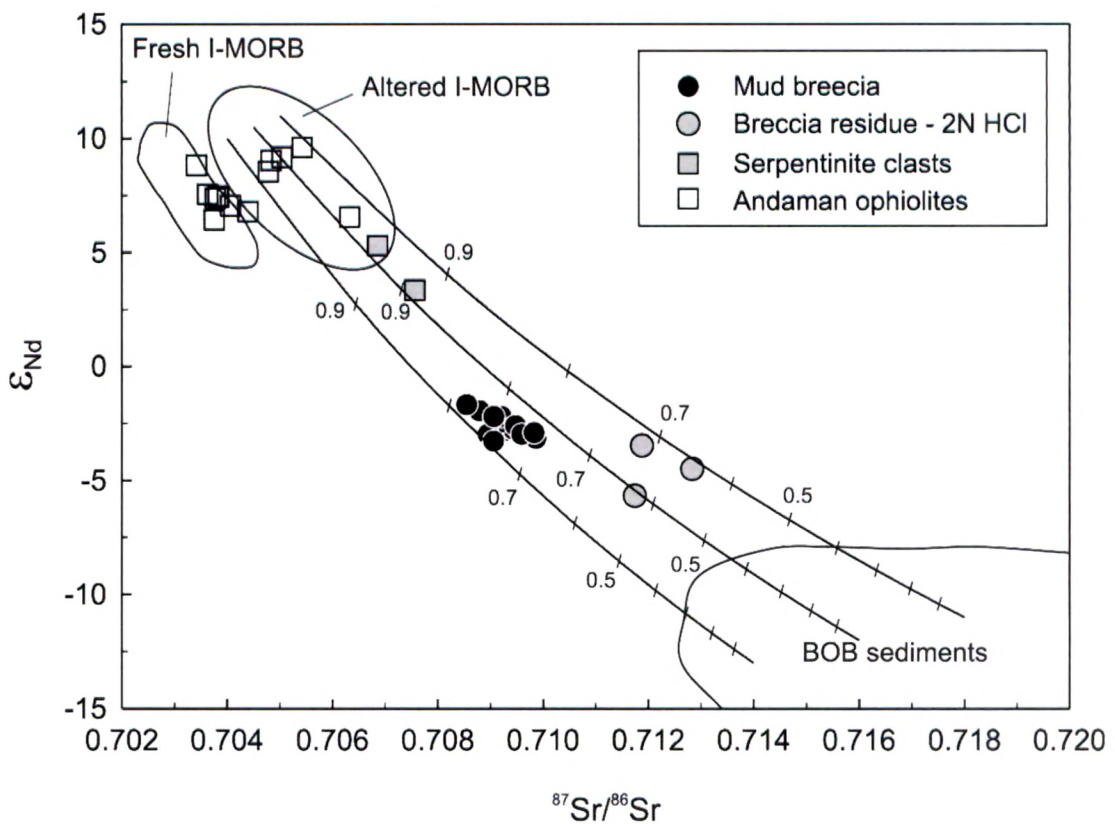


Fig.6.15: ϵ_{Nd} versus $^{87}Sr/^{86}Sr$ plot for mud matrix, HCl- residue fraction of mud matrix and serpentinite clast samples from mud volcanoes of Andaman Islands. The plot also contains data for rocks of Andaman ophiolites. The solid lines are two-component mixing curves between altered I- MORB and BOB sediments, with the numbers on them representing amount of the former in the mixture. Data sources: fresh Indian MORB (Mohaney et al 1989; Nauret et al 2006; Price et al 1986), Bay of Bengal (BOB) sediments (Derry and Frence-Lanord, 1996; Plank and Langmuir, 1998).

As major and trace element variations in the mud breccia hint at the possibility that it is slab derived, to confirm this we modelled their isotopic variations as a two components mixture of altered oceanic crust and trench sediments. Since altered oceanic crust of the slab represent altered MORB, altered Indian MORB was taken as one end member, whose $^{87}Sr/^{86}Sr$ is higher than that of I-MORB but ϵ_{Nd} is similar as Nd is resistant to seawater alteration. Interestingly, a large number of ophiolite samples from the Andamans plot within the field of altered I-MORB (Fig.6.15). The serpentinite clasts that accompanied the mud breccia too

plot within this field justifying our assumption (or choice of end-member composition). The second end-member was chosen to be the sediments from Bay of Bengal that most likely to be subducted beneath the Burma Plate along the Andaman Trench. Mixing curves were generated for three different pairs of end member compositions and compared with the observed data from mud breccia (Fig. 6.15) and it was found that the mud breccia in Andaman mud volcanoes do indeed represent the slab and has contributions of 70 - 80% from the altered oceanic crust and 20 - 30% of the trench sediments. This also confirms our earlier observation from clay mineralogy and major and trace element variations that mud breccia predominantly represents the mafic oceanic crust.

Through this study we not only have understood the origin of the mud breccia but also have now chemically characterized the slab sediments that get subducted at the Andaman Subduction Zone.

6.2.5 Origin of clasts

As discussed earlier, the clasts that accompanied the mud breccia and were violently ejected through the vents of mud volcanoes belong to the host rocks that overlie the main mud horizon. Most of the clasts we have observed and chemically analyzed belong to the Ophiolite Group and Mithakhari Group of rocks. Their chemistry (Table 5.1b) and isotopic compositions (Table 5.3b) attest to the above observations. The clasts from the ophiolites were mostly pillow lavas of various sizes, whereas serpentinite clasts that were more like compressed green coloured clay minerals did not appear to represent any of the rock units of the Ophiolite Group. Instead, their clay mineralogy (Fig. 5.3a), and major trace and isotope chemistry are similar to the mud breccia and hence, appear to have been derived from deep within the accretionary wedge – most likely from the mafic crust of the slab.

6.3 Origin and evolution of Barren Island Volcano

6.3.1 Inferences from field studies

The details of volcanological aspects of Barren Island (BI) volcano and our field observation are given in chapter-3. Here we list our major findings, based on field studies, on the evolution of the volcano.

I) We have classified the lava flows on the island into three groups stratigraphically, as precaldera, post caldera and modern formations, on the basis of the caldera forming event.

II) The prehistoric activity of the volcano (precaldera formations) is represented by lava-flows, lahars, pyroclastic fall and surge deposits along the roughly circular caldera wall.

III) The post caldera and modern eruptions have produced aa and blocky aa lava flows and tephra that occupy the central depression around the cinder cone. All these flows, except the most recent one of 2009-10, have taken the same route, through a breach in the caldera wall in the northeast, to reach the sea-where they form a lava delta. The most recent lava flows have taken a route through the northern section of caldera wall.

IV) For the first time we have identified and reported toothpaste lava flows on the island belonging to 1994-95 eruptions (Sheth et al. 2011).

V) The central cinder cone appears to be ~ 500m high above the sea level and is still growing with each eruption.

VII) From the field evidences it is apparent that the island is growing in size and central depression between the cinder cone and the

caldera wall is slowly getting filled with fresh ash and older ash washed off from top of caldera wall.

6.3.2 Inferences from petrography

The lava flows on BI are grayish black to brownish black and highly vesiculated basaltic rocks which show porphyritic texture with glassy ground mass and contain abundant phenocrysts of plagioclase, olivine and clinopyroxene. The rocks contain up to 47% crystals by volume. Plagioclase is extremely abundant as a phenocryst, commonly showing zoning or twinning, sometimes both. Many plagioclase phenocrysts are very well-developed euhedral, tabular crystals and contain large numbers of glass inclusions. Clinopyroxene phenocrysts show twinning and zoning. The zoning in the plagioclase crystals indicates incomplete equilibration with surrounding liquid. Luhr and Haldar (2006) have reported that some of the plagioclase and olivine megacrysts in BI lavas are not phenocrysts but xenocrysts, representing disaggregated troctolitic cumulate from a shallow magma chamber.

6.3.3 Geochemistry of lavas and ash beds

Clues from major and trace elements concentrations

In the absence of absolute chronology, we grouped the volcanics on Barren Island (BI) into three formations based on their relative chronology with respect to the caldera forming event as: precaldera, post caldera, and modern. All our interpretations below follow the above classification.

We classified the lavas from BI using their total alkalis (TA), $\text{Na}_2\text{O} + \text{K}_2\text{O}$ and silica (S) contents (Le bas et al., 1986). Figure 6.16 gives the results of this classification, which reveal that BI lavas, sampled by us, are subalkalic basalts or basaltic andesites. Interestingly, lavas of precaldera eruptions have wide range of compositions varying from basalt to high

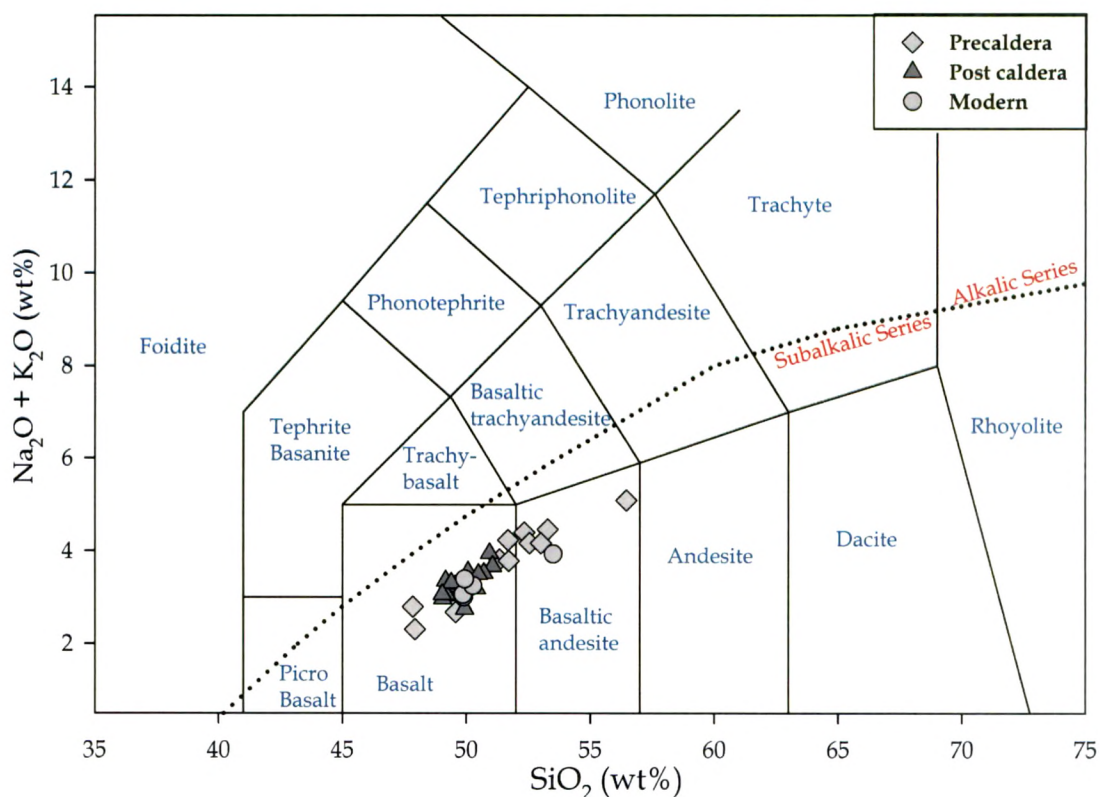


Fig. 6.16 Classification of lavas and ash beds from Barren Island based on total alkali vs. Silica variation (after La Bas et al; 1986). The samples are grouped according to their chronology with respect to the caldera forming event. The dashed line marks the boundary between alkalic - subalkalic series (Irvine and Baragar, 1971).

silica basaltic andesite, while the post caldera and modern lavas are mainly basaltic. The MgO content of all lavas ranges from 2.39 to 9.28 wt %, while their Mg number (Mg#) varies from 39 to 69.

In the AFM diagram (Fig. 6.17) the lavas of Barren Island plot very close the line that divides the tholeiitic series from the cal-alkaline series with most of the precaldera lavas falling within the tholeiitic. Modern lavas appear to be slightly calc-alkalic in nature, however, when we utilize the $\text{FeO}^T / \text{MgO}$ vs. SiO_2 plot (Fig. 6.18), it is quite clear that most of the lava flows are tholeiitic in nature. K_2O versus SiO_2 plot (Fig. 6.19) points out that BI lavas are derived from low to medium - K series magmas, and

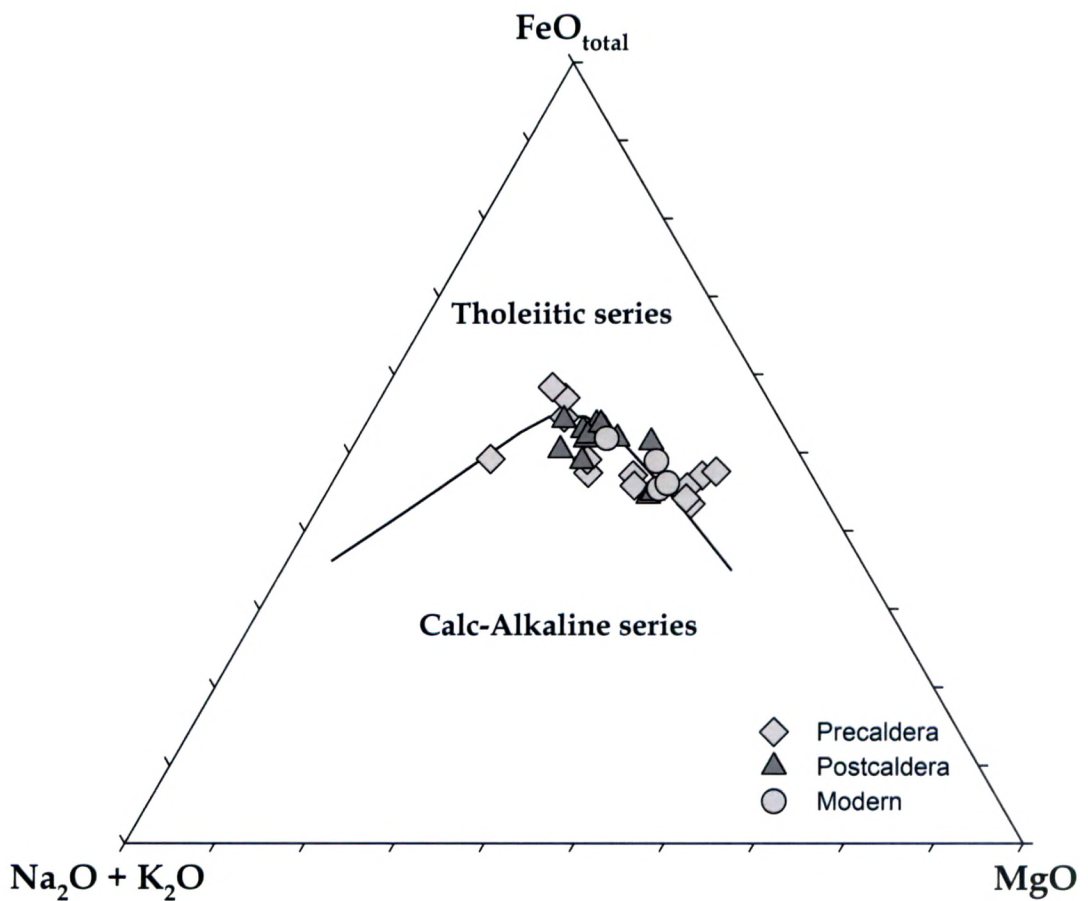


Fig. 6.17 AFM diagram for Barren Island lavas and ash beds. The boundary between the calc-alkaline field and tholeiitic field is after Irvine and Baragar (1971)

their Fe enrichment as seen in Fig. 6.18 is a result of early stage differentiation. The Differentiation trends are quite prominent in precaldera lavas in Fig. 6.18 and Fig. 6.19 and in major oxide variations against MgO in Fig. 6.20. It appears that a majority of precaldera eruptions belong to a single eruption and the lava flows were derived from a single parental magma. Lavas with lowest K_2O and $\text{FeO}^{\text{T}} / \text{MgO}$ with $\text{MgO} > 8$ (Figs. 6.18-6.20) belong to the precaldera formation and possibly are the most primitive lavas present on the island volcano. We believe that either one or more of these flows may actually represent the primary magma or compositionally much closer to it.

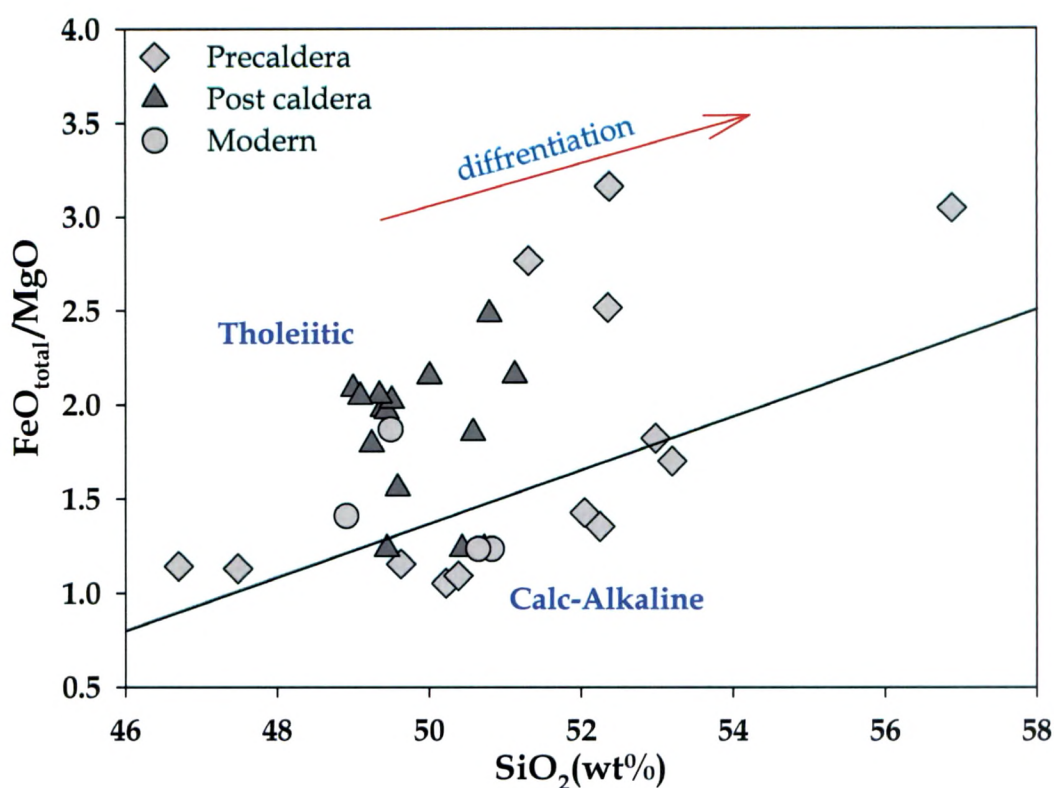


Fig. 6.18 FeO^T vs. Silica variation diagram of lavas and ash beds from Barren Island volcano (after Miyashiro, 1974), arrow represents differentiation trend

Evidences for fractional crystallization are observed in BI lavas (Fig. 6.20), when major oxides are plotted against MgO. Decreasing trends for CaO and SiO₂ and increasing trends for Al₂O₃ and K₂O (and Na₂O) could be attributed to crystallization of plagioclase, whereas decreasing FeO with MgO could point to Mg-rich olivine fractionation from the melts. Differentiation trends are much more prominent in trace element versus MgO plots (Fig. 6.21 and 6.22). Linear fractionation trends are observed for compatible trace elements like Cr, Co, Ni and Sc - which can be attributed to crystallization of olivine from the melt (Fig. 6.21). Once again these trends are quite prominent in precaldera lavas. No obvious trends are observed in incompatible trace element variations (Fig. 6.22). However, some rough decreasing trends are observed (with increasing MgO) in LREE of BI lavas and ash bed samples.

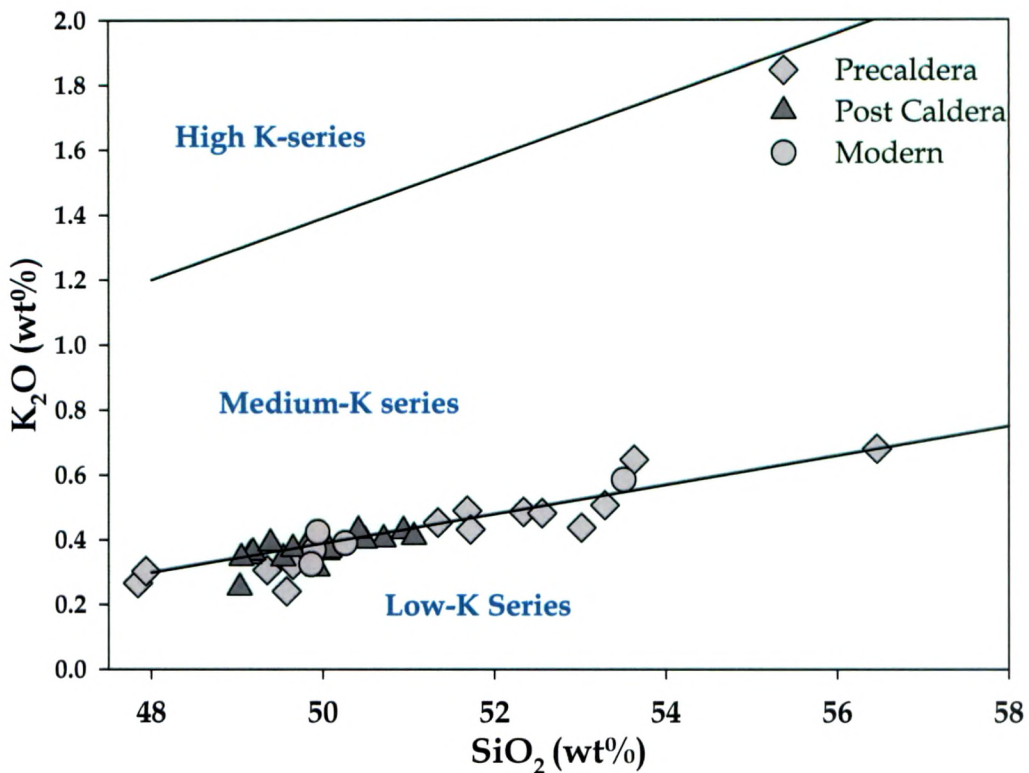


Fig. 6.19 Classification of lavas and ash beds from Barren Island based on K_2O vs. silica variation (after Le Maitre et al., 1989)

Summarizing the major oxide data it can be said that the lavas on the Barren Island Volcano are predominantly tholeiitic in nature and belong to high Al_2O_3 , low to medium-K magmas that are typical of island arc magmatism. Eruptions prior to caldera formation appear to have come from one batch of magma and have undergone extensive fractional crystallization, whereas postcaldera and modern eruptions possibly represent various batches of new magma entering into the magma chamber and the volcano's plumbing system.

Multiple incompatible trace-element patterns of Barren Island volcanics normalized to N-MORB are shown in Fig. 6.23. During subduction, the oceanic slab decarbonates and dehydrates to release fluids into the overlying mantle wedge. These fluids react with the mantle wedge and cause partial melting, which ultimately gives rise to lavas with

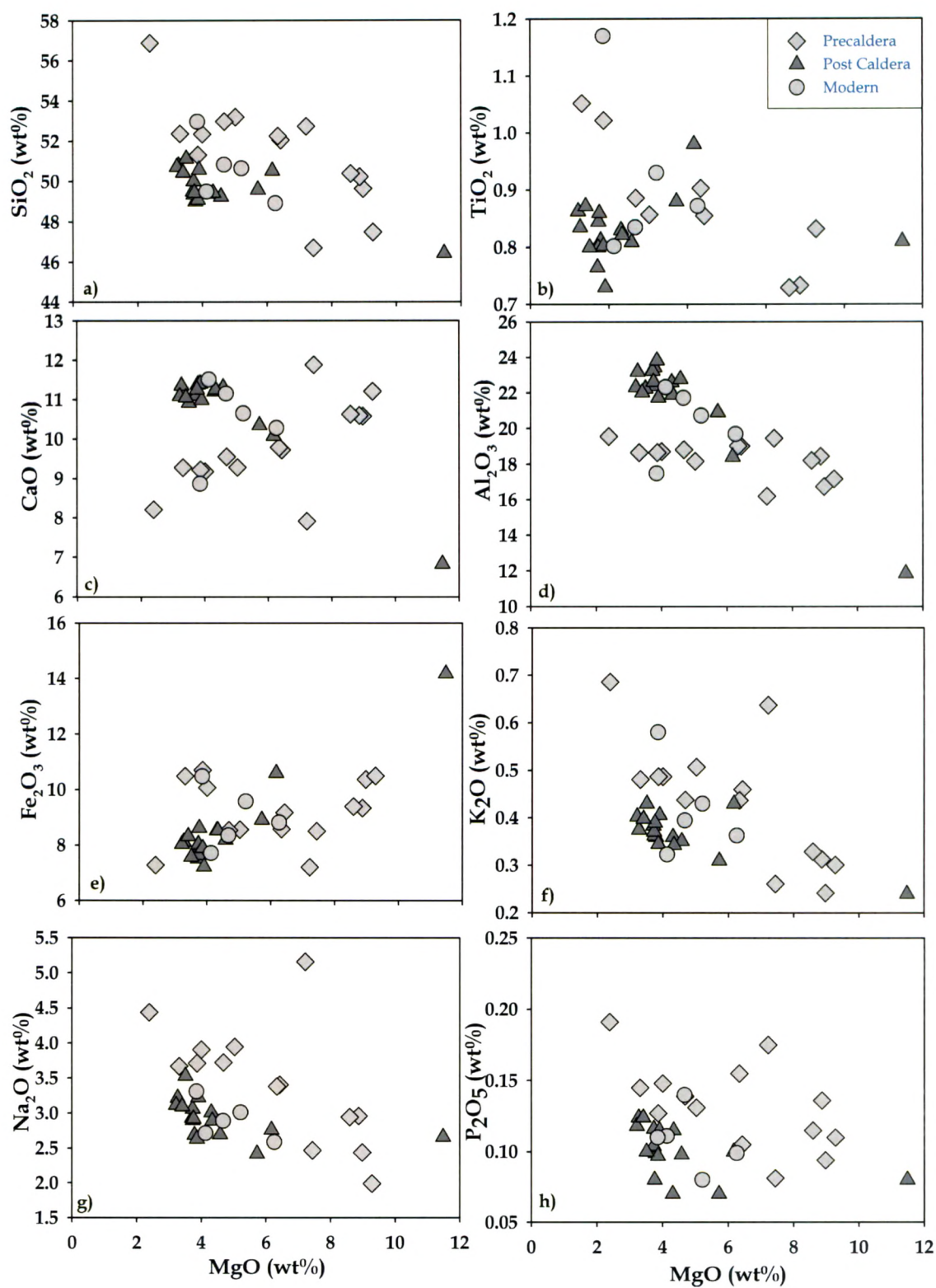


Fig. 6.20 Variation diagrams of various major oxide vs. MgO contents in lavas and ash beds of Barren Island.

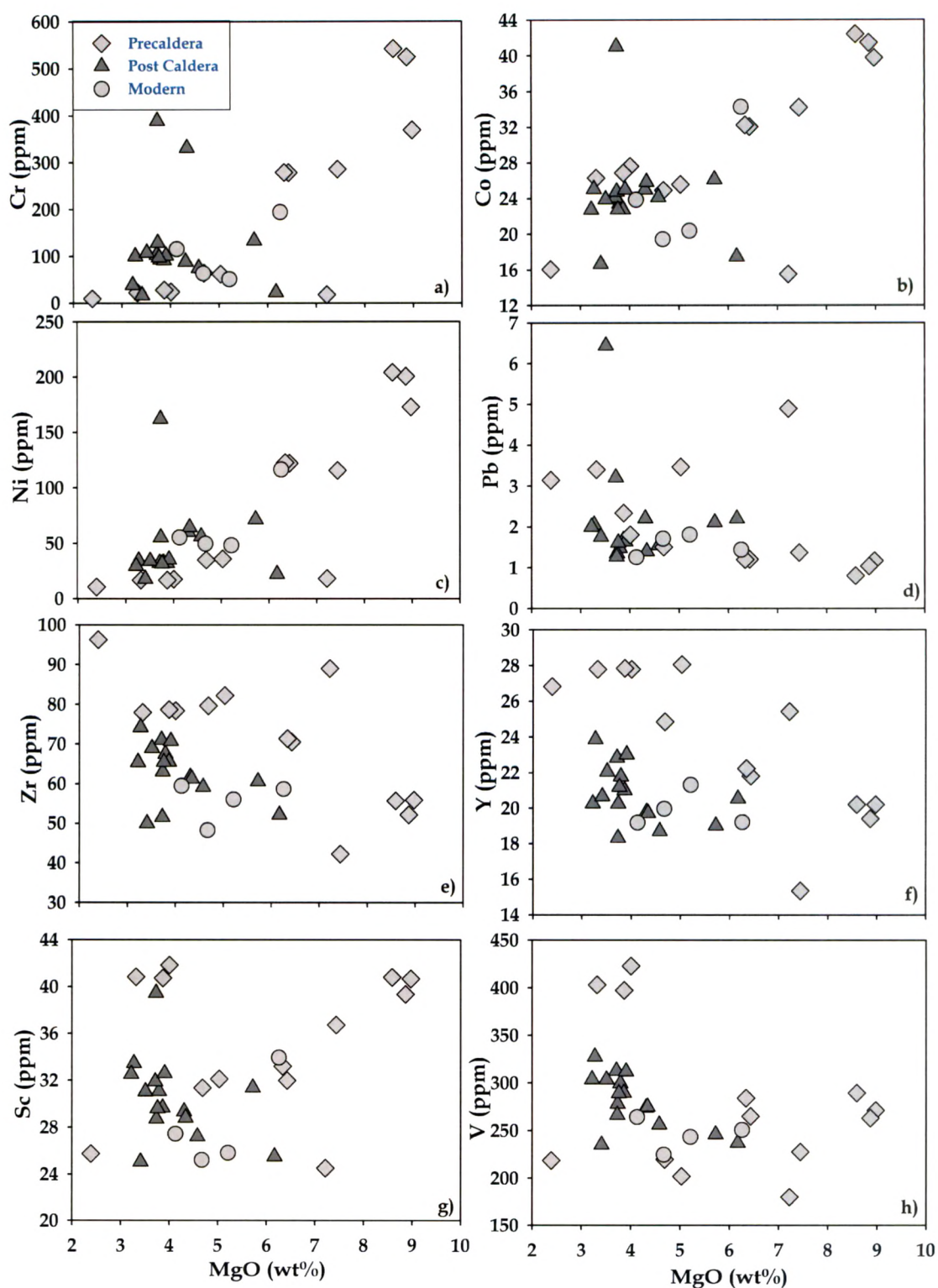


Fig. 6.21 Variation diagrams of various trace element concentrations vs. MgO contents in lavas and ash beds of Barren Island.

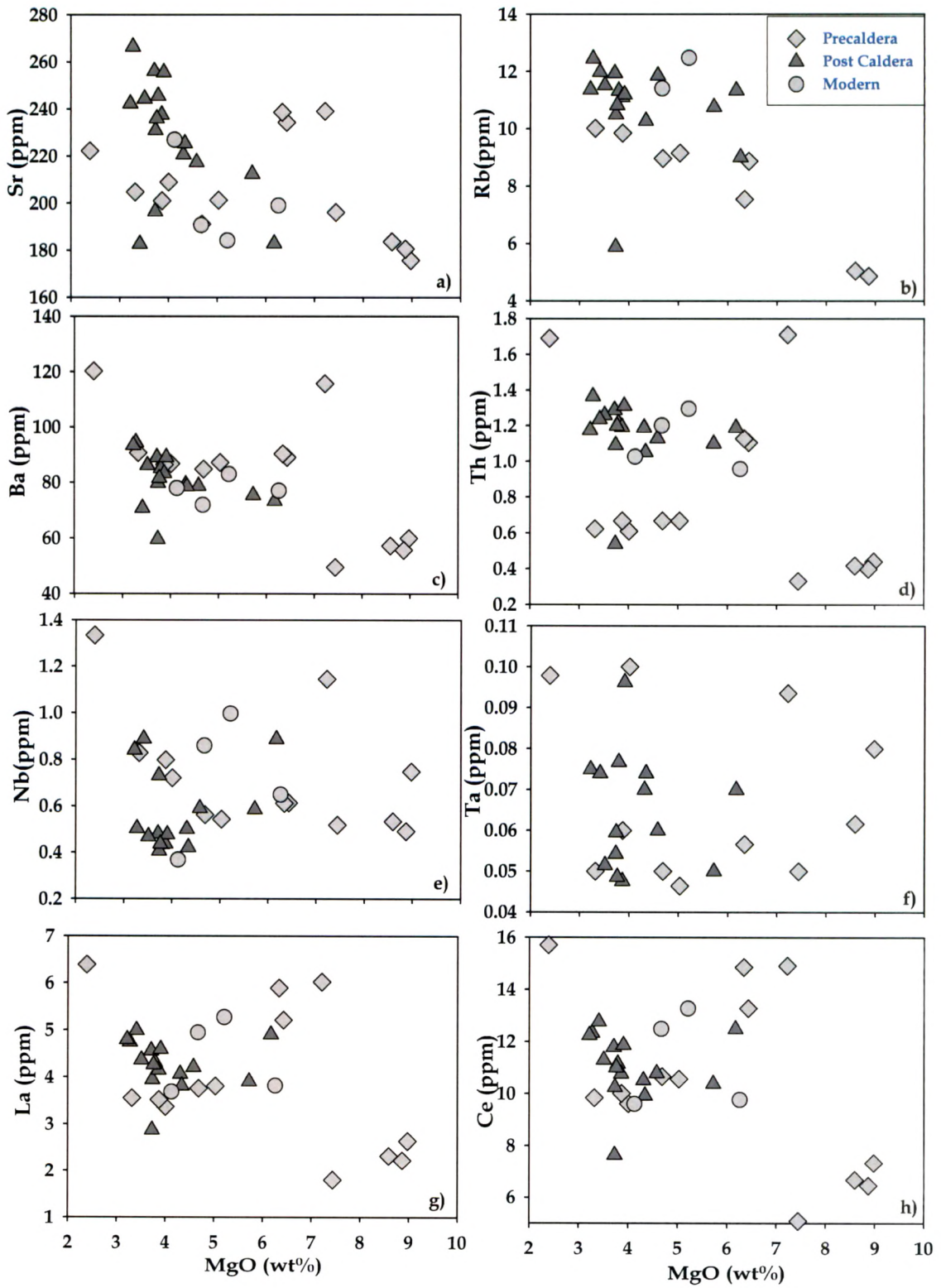


Fig. 6.22 Variation diagrams of various trace element concentrations vs. MgO contents in lavas and ash beds of Barren Island.

arc signatures. The different fractionation stages of the samples make it difficult for direct inter-comparison of chemistry of magma batches; however, general trends can be recognized. The modern and post caldera lava flows and ash beds show depleted characteristics as compared to precaldera lava flows and ash beds. The N-MORB normalized trace element patterns of BI lavas show typical characteristics of arc volcanics, such as the negative Nb and Ti anomalies and positive K, Ba and Pb spikes with lesser enrichment of Sr (Fig. 6.23). It can also be seen that the BI lavas roughly mimic the pattern of the E-MORB for most elements except for those characteristic arc signatures seen in Nb, Ta, Pb and Sr. Additionally, we also observe depletion of Ti in BI lavas.

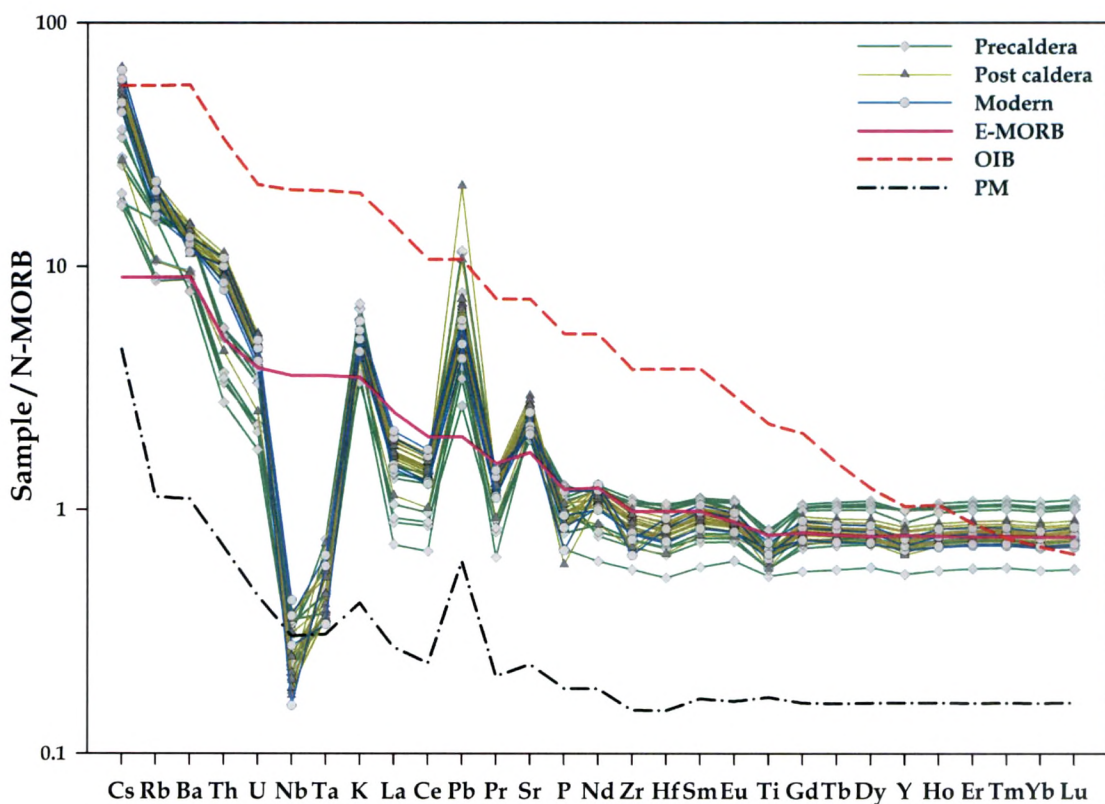


Fig. 6.23 N-MORB normalized incompatible trace element patterns of lavas of Barren Island. Normalizing values are from Sun and McDonough 1989. Also shown for comparison the patterns for global averages for Ocean Island Basalt (OIB), Primitive Mantle (PM) and Enriched MORB (E-MORB).

The magnitude of the anomalies mentioned above varies between samples, and nearly all show a small depletion in Ti with respect to the REE. The relative enrichments of Ba and Rb also vary in an unsystematic manner, as shown by the mafic lavas from precaldera samples. The depletion of Nb relative to LILE (large ion lithophile elements) can be attributed to two processes: I) the addition of an LILE enriched and Nb poor fluid component to the mantle wedge and/or II) the preferential retention of Nb in amphibole relative to other phases in the mantle source (Hawkesworth et al., 1993). Similar processes can be invoked for the general depletion of the high field strength elements (HFSE) Zr, Ti and Y with respect to LILE in BI lavas.

The chondrite normalized REE patterns of BI lavas (Fig. 6.24) appear to be almost flat, except for small enrichments/depletions in LREE. Interestingly, some samples from the precaldera formation that show slight depletions in LREE have similar patterns as seen in average N-MORB. Patterns shown by arc lavas from the Sunda- Banda subduction zone is much more enriched in LREE compared to BI lavas – clearly suggesting that the former are either highly evolved lavas or have had contributions from crustal contamination. The almost flat REE patterns of BI lavas clearly indicates that parental magmas for these were derived from high degree partial melts (>5%) from the mantle. These also suggest that the parental magma had little, if any, crustal contamination prior to their eruption.

Clues from radiogenic isotopic ratios: mantle source characteristics

The Sr and Nd isotopic compositions of Barren Island lavas and ash deposits show a very restricted variation compared to that in other arc magmatism in the region (Fig. 6.25). Isotopically these lavas are very primitive in nature and overlap with the field of MORB lavas (Fig. 6.25)

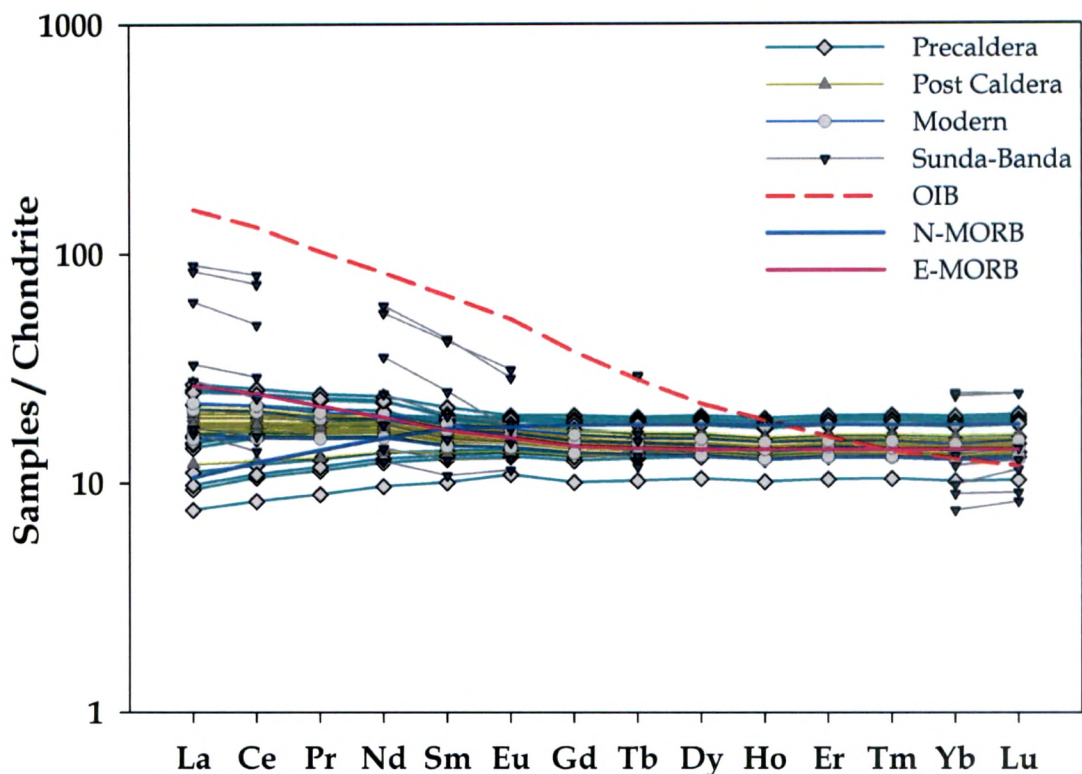


Fig. 6.24 Chondrite normalized rare earth element patterns for lavas of Barren Island, average OIB, average N-MORB and E-MORB and Arc lavas from Sunda-Banda subduction zone. Normalizing values are from Sun and McDonough, 1989; Data source for Sunda-Banda arc lavas are from Turner and Foden, 2001.

clearly suggesting that the mantle source for BI magma may not have been metasomatized to the extent one would expect for a mantle wedge in a ~100 Ma old subduction zone. The story from the Pb isotopic ratios is also similar as they show some of the lowest ratios observed in arc magmas. In the following paragraphs we attempt to understand the nature of the mantle source of BI magmas through the variations of their isotopic ratios and ratio of some useful trace elements.

Most models of magma petrogenesis at island arcs involve three main source components: I) the mantle wedge II) the subducting slab (oceanic crust and associated sediments); III) the arc lithosphere. The majority of island arc magmas are thought to originate in the mantle

wedge which has been inferred by several workers to be similar to the source of MORB (Ringwood, 1974, Ellam & Hawkesworth, 1988, Turner et al., 2003). In Andaman subduction zone, the slab is essentially the oceanic crust of Indian plate, and therefore for modelling purpose we consider Indian-MORB (I-MORB) as the unaltered mantle wedge and sediments of Bay of Bengal (BOB) as the unaltered sediments.

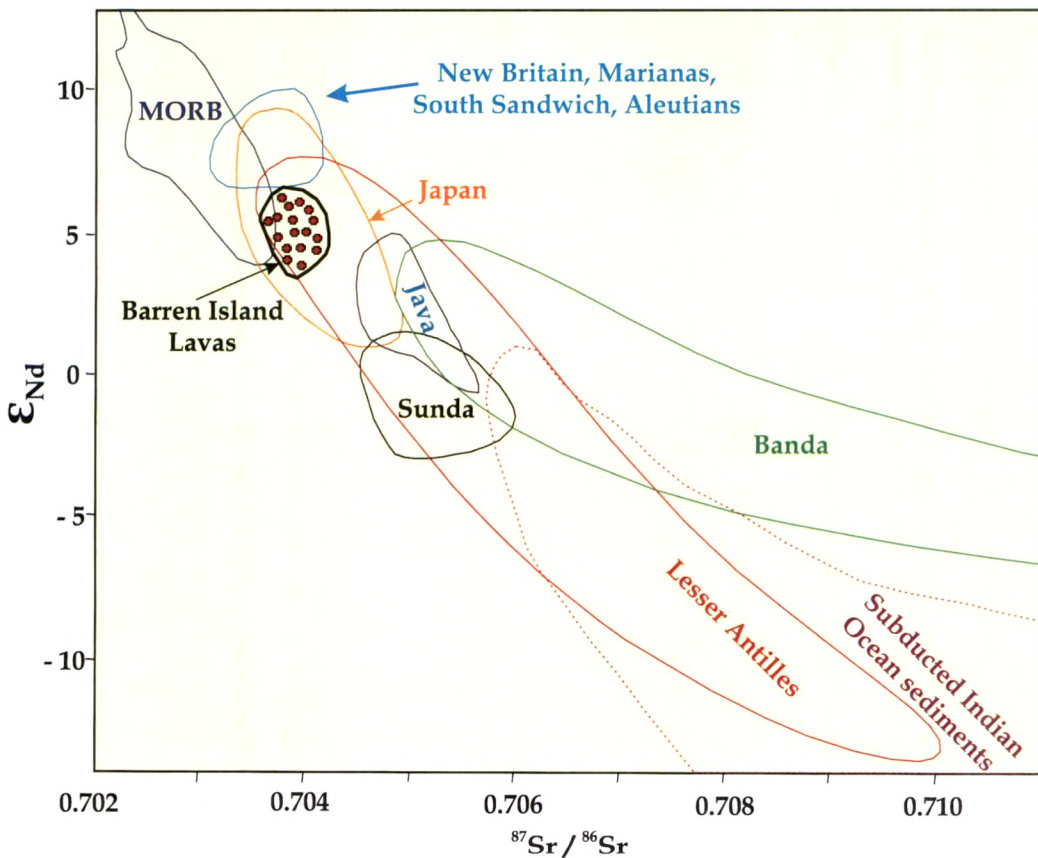


Fig. 6.25 $\epsilon_{Nd}(0)$ vs. $^{87}Sr/^{86}Sr$ plot for Barren Island volcanics. Fields for various other mantle derived rocks, arc lavas and ocean sediments are plotted for comparison. (Data sources: Wilson, 1989)

a) Slab fluids versus slab sediments

Experimental work (Tatsumi et al., 1986) and geochemical studies on arc lavas (McCulloch & Gamble, 1991) indicate that Nd is relatively immobile during slab dehydration (Kessel et al., 2005). Ba and Ce are more mobile in fluids compared to Th, which is an indicator of sediment

contribution. Th is preferred over K (which gives a better discrimination between different mantle components) because it is less mobile in aqueous fluids and hence more important in the study of subducted sediments (Pearce et al., 1992). The above characteristics of trace elements were the essence of our geochemical approach and we, therefore, have used to Ba/Th and Th/Ce versus $^{143}\text{Nd}/^{144}\text{Nd}$ variations in BI lavas to evaluate the contributions of slab derived fluids and sediments to the mantle wedge (Fig. 6.26a). Since we already have established that the mud breccia from the mud volcanoes of the Andamans represent the slab sediments that get subducted - their average compositions are considered here as the sediment end members. From the variations in BI lavas it is evident that the mantle wedge initially was affected by the fluids derived from the slab, as reflected in high Ba/Th at constant $^{143}\text{Nd}/^{144}\text{Nd}$ in early formed precaldera lavas. The source region was subsequently received contribution in form of particulate matter (sediments) from the slab sediments that affected both the isotopic ratios and Th content of the late precaldera, post caldera and modern lava flows.

The high Pb/Ce and low Nb/Zr ratios in precaldera lava flows also suggest that the precaldera lavas have imprints of fluid, whereas postcaldera and modern lavas have significant imprints of sediments. Comparing the $^{143}\text{Nd}/^{144}\text{Nd}$ versus Th/Ce of BI lavas with those of the arc lavas from Indonesia (Fig. 6.26b) we observed that the former appeared to have low contributions from slab derived materials, making them the most primitive amongst all the volcanoes in the greater Andaman – Sunda – Banda arc system.

b) Slab versus mantle wedge

To understand the slab versus wedge contributions to the magmas of Barren Island we have utilized a two and a three component mixing

models using different end-members of the Andaman Subduction Zone. Since Sr and Nd isotopes are powerful indicators of the composition of the sub-arc mantle and slab to mantle wedge transfer processes, we have utilized these ratios to understand the contributions from various end-members to the magmas.

Figure 6.27a shows simple solid-solid binary mixing curves between average Indian(I)-MORB source and a sediment source representing the subducting slab sediments. As discussed earlier mud breccias from mud volcanoes of Andamans are deemed to represent the sediments of the subducting slab. Mixing curves are generated for different Sr/Nd ratios. Addition of 10-20% average bulk mud sediments to I-MORB produces a curve that passes through the most isotopically primitive precaldera lavas (Fig. 6.27a). The isotopic ratio variations in post caldera and modern lavas cannot be explained by a simple two components mixing. Therefore, we invoked a three component mixing model for isotopic ratios involving I-MORB representing the mantle wedge, altered oceanic crust (basaltic) representing the slab crust and mud breccia representing slab sediments. Interaction of seawater with basalt produces significant chemical and isotopic changes (Hart et al., 1974, White & Patchett, 1984). For the altered oceanic crust end-member, we considered the serpentinite clasts found in the mud breccia since they represent material derived from the slab deep in forearc. The model curves are presented in Fig. 6.27(b) along with the data from BI lavas. As can be seen, the precaldera lavas contain more of I-MORB end-member compared to others indicating their primitive nature. These lavas also have higher contributions from altered oceanic crust compared to sediments, whereas the post caldera and modern lavas have higher contributions from sediments – which support our earlier inference based on trace element geochemistry.

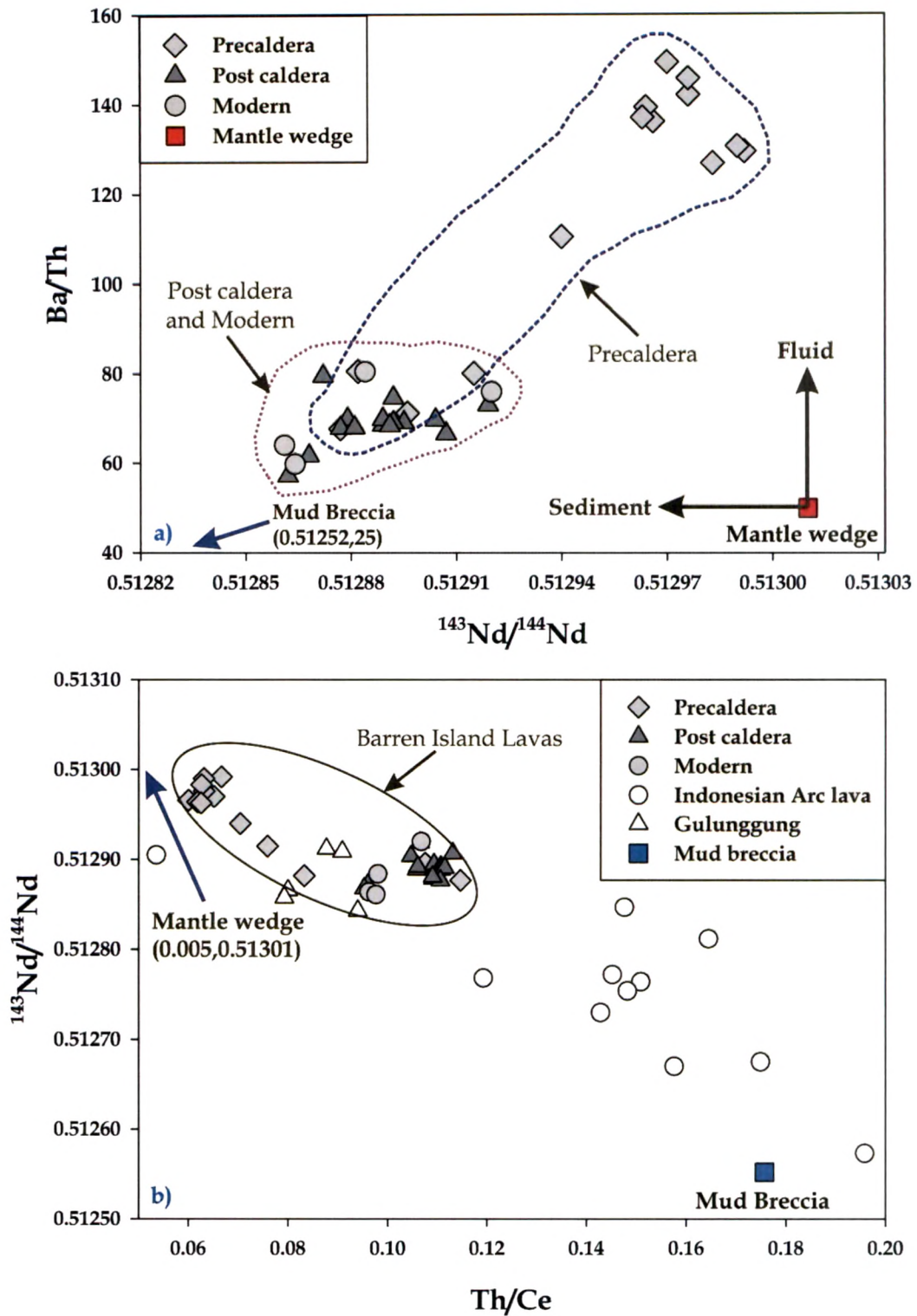


Fig. 6.26(a) $^{143}Nd/^{144}Nd$ versus Ba/Th for Barren Island lavas (b) Th/Ce versus $^{143}Nd/^{144}Nd$ plot for Barren Island lavas and Indonesian Arc volcano lavas (Turner and Foden 2001), Mantle wedge (I-MORB) : Rollinson, 1993

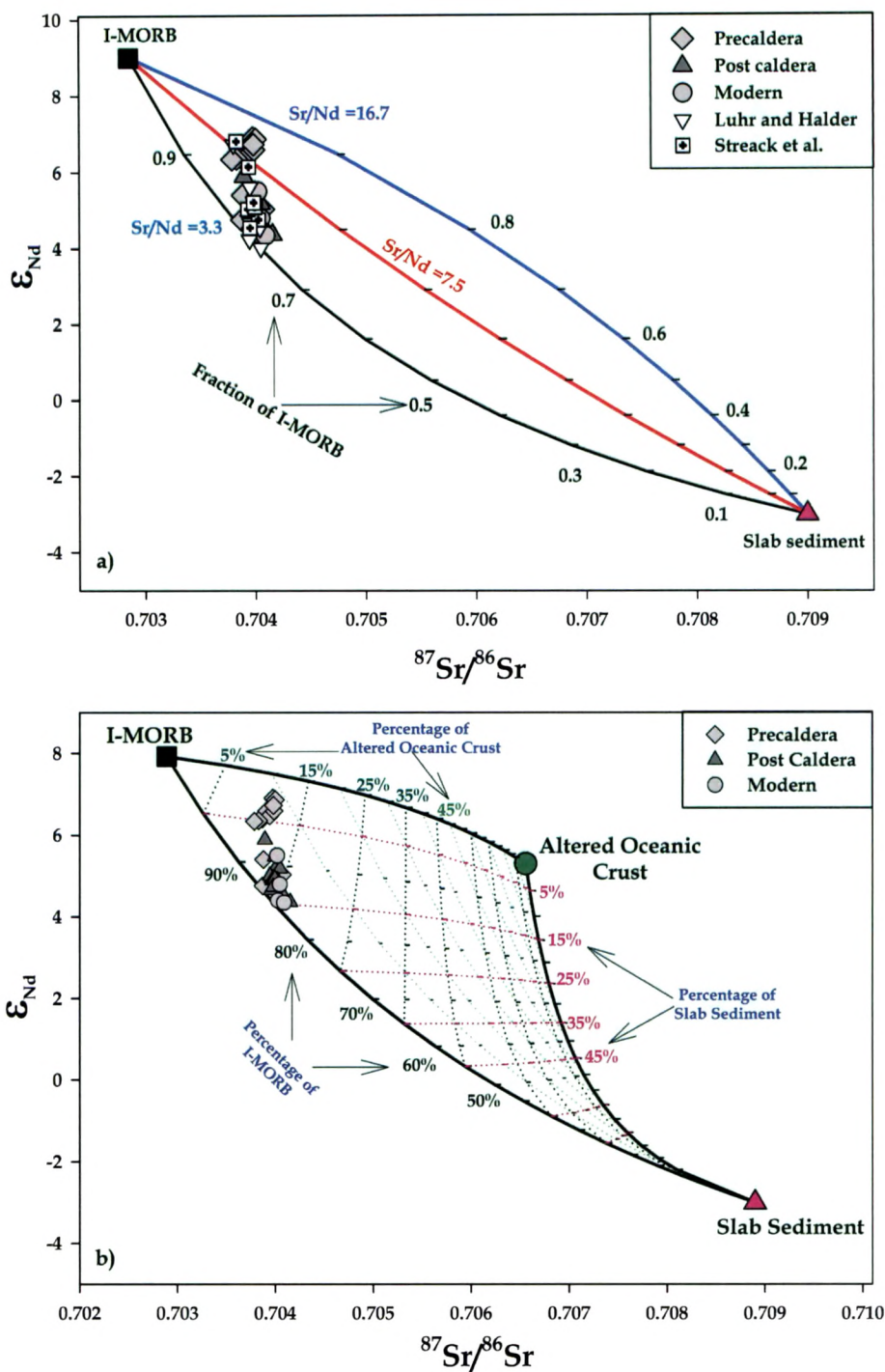


Fig.6.27 (a) ϵ_{Nd} vs. $^{87}Sr/^{86}Sr$ of BI lavas compared with two components mixing curves, where I-MORB & slab sediments are the two end members. Mud breccia are considered to represent the slab sediments (b) The same data, as in (a) compared with three components mixing curves involving I-MORB, slab sediments and altered oceanic crust as end members. Source for I-MORB: Nauret et al. 2006, and Altered oceanic crust: serpentinite clasts from Andaman mud volcanoes and slab sediments: mud breccia from mud volcanoes of Andamans

The Pb isotopic data can give first impression of the identity of the end-members involved in the magma genesis, since, unlike in Sr and Nd isotopic plots, two component mixing lines in Pb - Pb diagrams are straight and are independent of slab to mantle transfer processes. In the Pb isotopic variation diagram, the Pb isotopic ratios in BI lavas show linear arrays and fall well above the Northern Hemisphere Reference Line (NHRL) clearly suggesting Pb contribution from two distinct mantle sources (Fig. 6.28). One of the sources is a non-radiogenic source, most likely the pristine Andaman mantle wedge similar to the source of I-MORB, and the other appears to be a source affected by radiogenic Pb derived from the slab – most likely from subducted Indian Ocean sediments. In addition, the scatter Pb isotopes data for BI lavas suggests variability in the subducted components to the mantle source.

Mantle melting and magma generation

a) Degree of melting

Trace element variations are good indicators of degree of melting within the mantle; therefore, we modelled their behaviour in a forward manner and attempted to simulate the observed concentrations in the BI lavas in order to determine the amount of melting for various magma batches.

To predict the concentration of an element in the melt produced by partial melting of lherzolite mantle affected by metasomatism (similar to a mantle wedge affected by fluids from the slab), we used the Rayleigh fractionation melting (non-modal) formulations of Shaw (1970). According to this model the concentration of an element in the aggregate melt is given by:

$$\overline{C}_L = \frac{C_o}{F} \left[1 - \left(1 - \frac{PF}{D_o} \right)^{\frac{1}{P}} \right] \quad (6.6)$$

Where \overline{C}_L = Concentration in aggregate melt after the melting is over

C_o = Concentration in the source rock at time t=0

D_o = Initial bulk distribution coefficient = $\sum X_o^i K_o^i$, where

X_o^i = Fractional abundance of minerals in the source

K_o^i = Mineral-melt partition coefficient

P = Bulk distribution coefficient for the melt = $\sum p^i K_d^i$

Where p^i = fractional abundance of mineral in the melt

F = Fraction of melt produced

For the model calculations we assumed the following mineralogy for the source: olivine = 60%; ortho-pyroxene = 20%; clino-pyroxene = 14%; garnet = 5%; amphibole = 1%. And since this model deals with non-modal melting, we assumed the following percentage of minerals going to the melt: olivine = 10%; ortho-pyroxene = 10%; clino-pyroxene = 33%; garnet = 39%; amphibole = 8%. Amphibole in the source signifies the presence of fluids in the source and garnet indicates deeper origin for the magma. The trace element concentrations for the mantle wedge were calculated assuming that the source for BI lavas was made up of: 90 % lherzolites, 8% altered oceanic crust and 2% slab sediments. These contributions are derived from the three components mixing model discussed earlier – based on Sr and Nd isotopic ratios. The trace element concentrations were taken from Kimura et al. (2010) and the compositions for BI source were determined by mixing the above three members as per their deemed contributions. The K_d (partition coefficients) values for

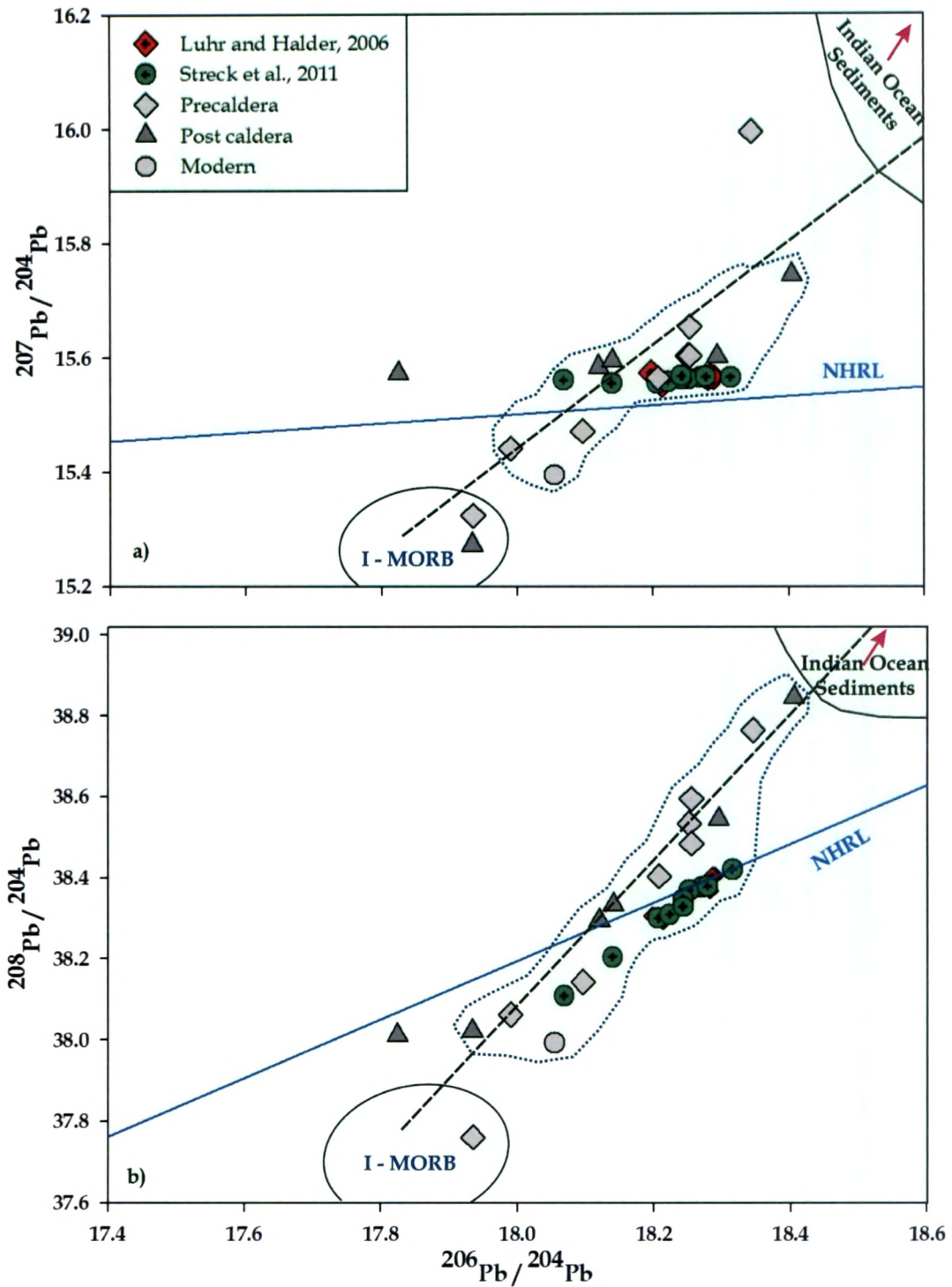


Fig. 6.28 (a) Plot of $^{207}\text{Pb}/^{204}\text{Pb}$ vs. $^{206}\text{Pb}/^{204}\text{Pb}$ (b) Plot of $^{208}\text{Pb}/^{204}\text{Pb}$ vs. $^{206}\text{Pb}/^{204}\text{Pb}$ of Barren Island lavas. NHRL (North Hemisphere Reference Line) is after Hart (1984). Data source: I-MORB: Nauret et al. 2006, Indian Ocean sediments: Plank and Langmuir (1998). The dashed lines represent rough mixing trends.

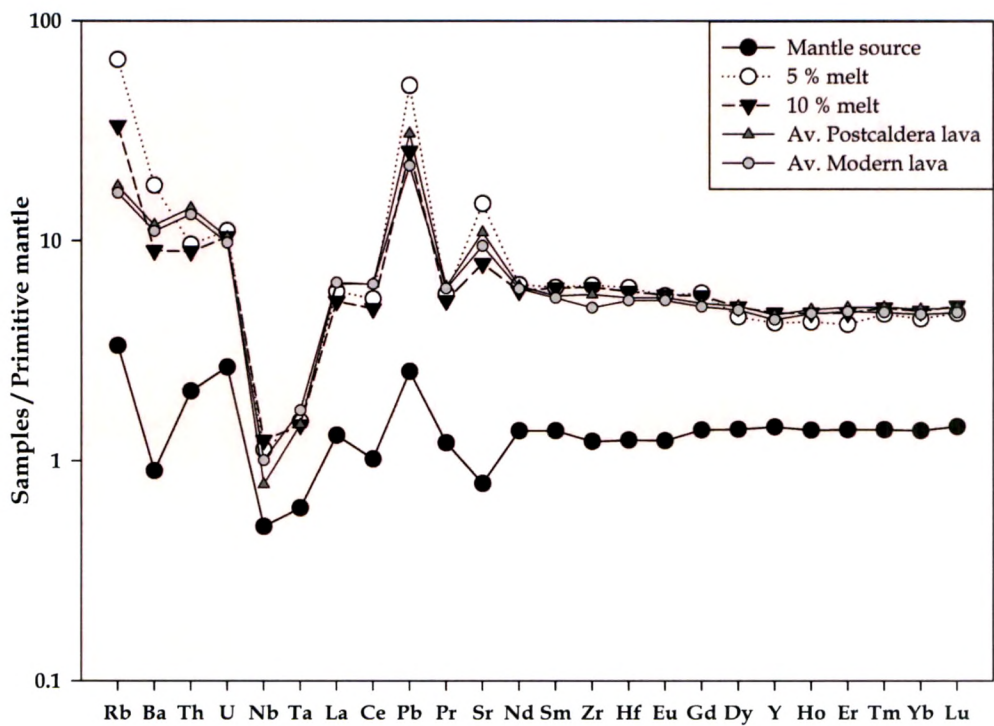
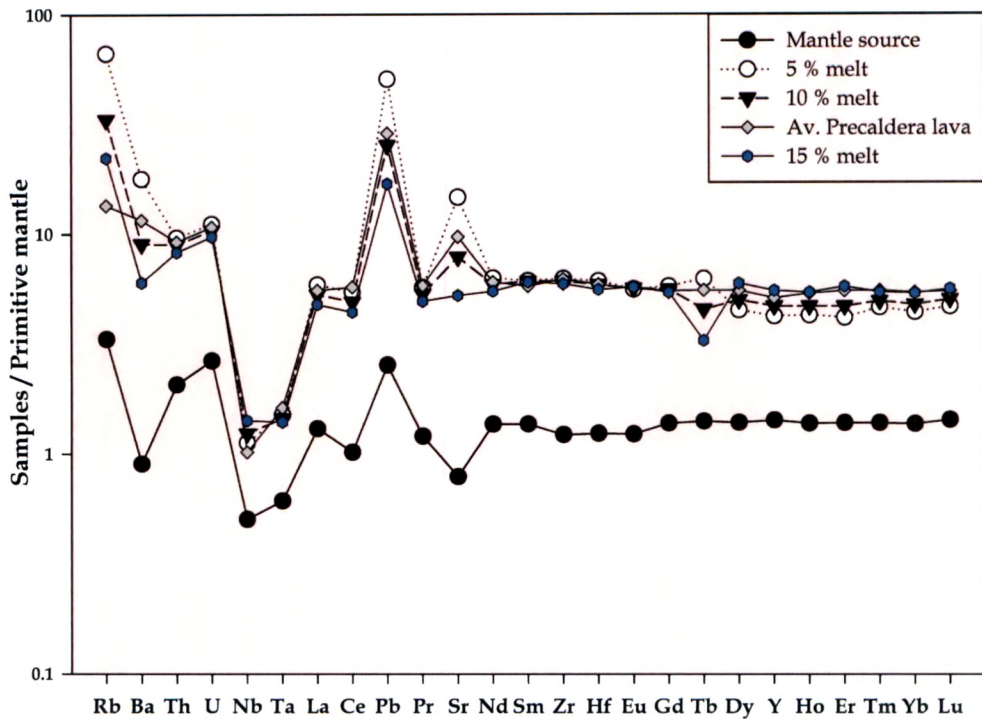


Fig. 6.29 Primitive mantle normalized incompatible trace element patterns in lavas from Barren Island compared with fractional melting model generated patterns (see text for discussion) a) Average precaldera lava is compared with the model curves b) Average postcaldera and modern lavas are compared with model curves

basaltic systems were taken from the GERM (Geochemical Earth Reference Model) website at: (<http://www.earthref.org/GERM/>).

Model trace element patterns were generated for various degrees of melting (F) and compared with the observed data for precaldera, post caldera and modern lava flows of the Barren Island Volcano (Fig. 6.29). To negate the effect of fractional crystallization (if any) on the trace element contents of these lavas (which are essentially whole rock data), average concentrations were considered for comparison (Fig. 6.29). The model remarkably reproduced the patterns observed in these lavas including the typical subduction zone signals in the elements like Nb, Ta, Pb and Sr. The most interesting observation is the replication of Sr – enrichment, in spite of the fact that the source rock is depleted in it. According to the model estimates the precaldera lavas have been produced from magma(s) that represents 5 -15% of parental melting of the mantle wedge, whereas the post caldera and modern lavas have been derived from magmas those represent 5 - 10% of parental melts of the mantle wedge.

b) Depth of melting

Determining the depth at which BI magmas have been generated in the mantle wedge is one of the most interesting questions related to the understanding the evolution of the volcano. The fact that our earlier models did suggest presence of garnet in the source of these lavas points to a deeper (>90 km) source (e.g., Herzberg et al. 2000). However, considering that mantle wedge may not exactly represent a normal asthenospheric mantle, we may need to use independent methods to determine presence of garnet and hence, the depth of melt generation.

Ratios of heavy rare earth elements (HREE) can provide some insight into the depth of melting in the mantle, because they are sensitive

indicators of garnet in the source. Once again, using a forward Rayleigh non-modal fractional melting (Shaw, 1970) as discussed earlier we generated model melts in a chondrite normalized $(Yb/Sm)_n$ vs. $(Tb/Yb)_n$ plot varying the amount of garnet in the source and the fraction of melt produced (Fig. 6.30). As done before, the elemental contents of the source were calculated assuming the source to be 90% lherzolites + 8% altered oceanic crust + 2% subducted sediments. The model curves were compared with the observed data for lavas (Fig. 6.30). The results of this modelling effort suggest that the grid for 5 - 15% fractional melting and 20 - 50% garnet in the source can explain the observed data. Interestingly, this model too suggests similar melting fractions as predicted earlier: 5 - 10 % for generation of precaldera lavas and 5 - 15 % for generation of

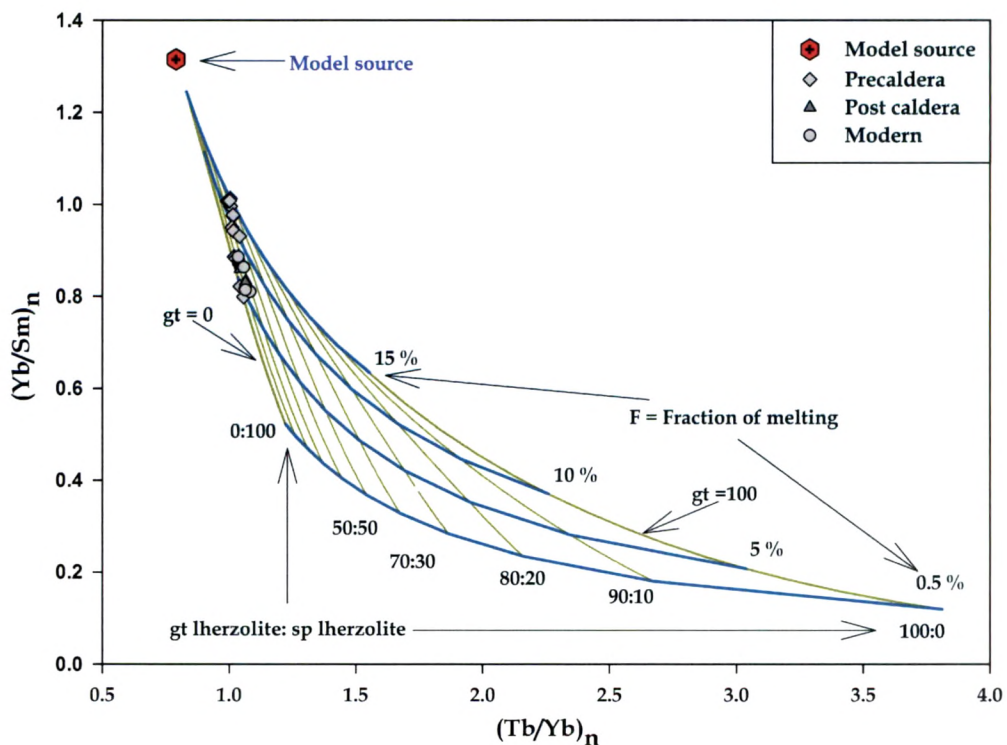


Fig 6.30 Chondrite normalized $(Tb/Yb)_n$ vs. $(Yb/Sm)_n$. The grid indicates the range of model melt compositions provided by 0.5%, 5%, 10% and 15% of aggregated fractional melting of a mantle wedge in which melting occurs in presence of garnet (spinal:garnet varies from 0 - 100%). See text for detailed discussion. Normalizing values are from Sun and McDough (1989)

post caldera and modern lavas. In summary, we can conclude that some of the lavas of the Barren Island Volcano are indeed derived from deep within the mantle wedge where garnet is a stable phase. Such a depth might exceed 90-100 km within the mantle wedge.